1 **Long-term ecological changes in Mediterranean mountain lakes linked to recent**

2 **climate change and Saharan dust deposition revealed by diatom analyses**

3

4

5 Carmen Pérez-Martínez[1,2], Kathleen M. Rühland[3], John P. Smol[3], Vivienne J. Jones[4]

6 and José M. Conde-Porcuna[1,2]

7

8 [1]Institute of Water Research, University of Granada, 18071-Granada, Spain

9 [2]Department of Ecology, Faculty of Science, University of Granada, 18071-Granada,

10 Spain

11 [3]Paleoecological Environmental Assessment and Research Lab (PEARL), Department

12 of Biology, Queen's University, Kingston, ON K7L 3N6, Canada

13 [4]Environmental Change Research Centre, Department of Geography, University

14 College London, Pearson Building, Gower Street, London, WC1E 6BT, U.K.

15

16 Corresponding author: Carmen Pérez-Martínez, cperezm@ugr.es

17

18

19

Highlights

- Diatom composition changes were linked to both climate change and atmospheric Saharan Ca input

- Decreasing lake water turbulence and volume occurred throughout the 20th century

- Increased aridity in Sierra Nevada lake-catchment ecosystems since the 1960s

- Post-1960 alkalinization of lakes linked to Saharan Ca input and climate change

- Timing of diatom responses differs from those recorded for sedimentary chlorophyll-*a* and Cladocera

Abstract

Anthropogenic climate change and the recent increase of Saharan dust deposition has had substantial effects on Mediterranean alpine regions. We examined changes in diatom assemblage composition over the past ~180 years from high-resolution, dated sediment cores retrieved from six remote lakes in the Sierra Nevada Mountains of Southern Spain. In all lakes, changes in diatom composition began over a century ago, but were more pronounced after ~1970 AD, concurrent with trends in rising regional air temperature, declining precipitation, and increased Saharan dust deposition. Temperature was identified as the main predictor of diatom assemblage changes, whereas both Saharan dust deposition drivers, the Sahel precipitation index and the winter North Atlantic Oscillation, were secondary explanatory variables. Diatom compositional shifts are indicative of lake alkalinization (linked to heightened evapoconcentration and an increase in calcium-rich Saharan dust input) and reduced lake water turbulence (linked to lower water levels and reduced inflows to the lakes). Moreover, decreases in epiphytic diatom species were indicative of increasing aridity and the drying of catchment meadows. Our results support the conclusions of previous chlorophyll-*a* and cladoceran-based paleolimnological analyses of these same dated sedimentary records which show a regional-scale response to climate change and Saharan dust deposition in Sierra Nevada lakes and their catchments during the 20th century.. However, diatom assemblages seem to respond to different atmospheric and climate-related effects than cladoceran assemblages and chlorophyll-*a* concentrations. The recent impact of climate change and atmospheric Saharan deposition on lake biota assemblages and water chemistry, as well as catchment water availability, will have important implications for the valuable ecosystem services that the Sierra Nevada provide.

57

60

1. Introduction

Mountain lakes are among the most sensitive ecosystems to be affected by climate change (Rogora et al., 2018; Moser et al., 2019), responding both directly (lake dynamics) and indirectly (mediated by the watershed and atmospheric inputs) to regional warming. Mediterranean high-mountain ecosystems have been identified as being particularly susceptible to anthropogenic climate change (Nogués-Bravo et al., 2008; Lionello, 2012). This is partially associated with the increased risk of summer drought in this region (Beniston, 2003) caused by the rise in mean summer air temperature and a reduction in annual precipitation (Nogués-Bravo et al., 2012) that collectively affect snow accumulation in low latitudes areas of Europe (Sánchez-López et al., 2015). Declining snow accumulation and earlier snowpack melt may, in turn, affect mountain ecosystem hydrology (Gobiet et al., 2014), biogeochemical processes in soil and water (Magnani et al., 2017, Preston et al., 2016) and species composition, phenology and structure (Grabherr et al., 1995, Steinbauer et al., 2018). A better understanding of Mediterranean mountain lake ecosystem responses to recent environmental change can strengthen our ability to forecast and mitigate the deleterious effects of recent climate change.

In addition to climate change, the southernmost regions of the Mediterranean are influenced by substantial atmospheric deposits of Saharan dust (Lequy et al., 2012; Pey et al., 2013), particularly during the spring-summer period. The amount of Saharan dust exported to the atmosphere has increased exponentially in recent decades as a consequence of droughts in North Africa (Prospero and Lamb, 2003), human-induced desertification (Moulin and Chiapello, 2006), and the expansion of commercial agriculture in the Sahel region (Mulitza et al., 2010). Saharan dust contains high amounts of phosphorus (P) and calcium (Ca), among other elements (Loÿe-Pilot et al.,

86 1986; Morales-Baquero et al., 2013), with substantial effects on terrestrial and aquatic

87 ecosystems (Rodá et al. 1993; Ridame and Guieu, 2002). For example, Morales-

88 Baquero et al. (2006) and Pulido-Villena et al. (2006) measured an input of 0.12-0.2 kg

89 ha^{-1} y^{-1} of total P and 12.1-19.3 kg ha^{-1} y^{-1} of Ca to the Sierra Nevada area (Spain).

90   The Sierra Nevada (southeast Spain) is the southernmost mountain range in

91 Europe (Fig. 1) and is one of the most important biodiversity hot spots in Europe. Its

92 summits support the highest plant biodiversity in the Mediterranean area with a high

93 rate of endemism (Blanca et al., 1998; Myers et al., 2000), but currently these plants are

94 experiencing an increased risk of climatic stress (Blanco-Pastor et al., 2013). This

95 Mediterranean mountain range has responded rapidly to recent warming with the

96 disappearance of permanent ice from the highest north-facing cirques (Oliva et al.,

97 2016). A trend in declining mean annual rainfall (Ruiz-Sinoga et al., 2011) and a

98 reduction of snow and ice cover since the 1960s (Pérez-Palazón et al., 2015) has

99 become more pronounced since the twenty-first century (Bonet et al., 2016).

100   In Sierra Nevada there are approximately 50 small alpine lakes and numerous

101 peat bogs situated between ~2,800 and 3,100 m asl. Limnological studies undertaken

102 over the past few decades have shown that water levels and temperature of these high

103 altitude lakes are affected by interannual differences in air temperature and precipitation

104 (García-Jurado et al., 2011; Villar-Argaiz et al., 2001), affecting plankton biomass and

105 nutrient availability (Barea-Arco et al., 2001; Morales-Baquero et al., 2006; Pérez-

106 Martínez et al., 2013), as well as epilithic diatom communities (Sánchez-Castillo et al.,

107 2008). In contrast to many other regions of the Northern Hemisphere, the Sierra Nevada

108 area is not particularly affected by acid deposition (Morales-Baquero & Pérez-Martínez,

109 2016), but rather by Ca and P-rich dust transported from the Sahara. Saharan dust

110 deposition has been shown to affect lake water nutrient and Ca concentration,

chlorophyll-*a* and the pool of dissolved organic matter (Morales-Baquero et al., 2006; Pulido-Villena et al, 2006; Mladenov et al., 2011), as well as bacterial growth and algal bacterial trophic interactions (Reche et al., 2009; González-Olalla et al., 2018) in these lakes.

In previous paleolimnological studies using sediment cores from six Sierra Nevada lakes, Jiménez et al. (2018) showed an increase in sedimentary chlorophyll-*a* (which includes its main diagenetic products) and changes in cladoceran assemblages from the mid-twentieth century onwards, whilst Jiménez et al. (2015, 2019) tracked changes in chironomid assemblage, sedimentary pigment composition, and catchment plant development in Río Seco Lake. Collectively, the results from these studies indicate a regional-scale response of Sierra Nevada lakes and their catchments to both 20th century climate change and increased Saharan dust deposition. Despite essential limnological research conducted during the last four decades, surprisingly little is known about the species-level responses of primary producers to recent environmental changes in Sierra Nevada lakes. Diatoms are powerful indicators of nutrients, pH, and alkalinity (Smol, 2008) and have been used extensively in paleolimnological studies to reconstruct past climatic and environmental fluctuations (Battarbee et al. 2010; Sochuliaková et al., 2018). Numerous studies in the Mediterranean Sea (e.g. Ridame and Guieu, 2002; Marañón et al., 2010; Gallisai et al., 2014) have reported that nutrient enrichment from Saharan dust deposition have had notable effects on marine phytoplankton growth and species composition. In contrast, the effects of Saharan dust input on freshwater primary producers is poorly understood, with only a few studies completed in Spanish mountain lakes. Camarero and Catalan (2012) in Pyrenees and Morales-Baquero et al. (2006) in Sierra Nevada analyze the effect of Saharan atmospheric phosphorus input on phytoplankton nutrient limitation whereas the

paleolimnological studies ofJiménez-Espejo et al. (2014) and Jiménez et al. (2018) analyze the long-term effect of sahara dust deposition on Sierra Nevada lake primary production and cladocerans. Here, we expand on the Jiménez et al. (2018) cladoceran study and examine high-resolution dated diatom records from the same six Sierra Nevada lakes to determine whether lower trophic levels (primary producers) have also responded to increased Saharan dust deposition and climate change over the past ~180 years. We anticipate that the recent limnological changes observed in Sierra Nevada lakes will be clearly expressed in our dated diatom records.

In this diatom-based paleolimnological study we address the following questions: (1) Has diatom assemblage composition changed over the past ~180 years? (2) Can changes in the diatom record be linked to regional climate and Saharan dust input? (3) How does the nature and timing of diatom changes compare to changes in other proxies (cladocerans, and chlorophyll-*a*) previously examined from these same sedimentary cores by Jiménez et al. (2018)?

2. Materials and methods

2.1. Site description

In the Sierra Nevada Mountains (Granada, SE Spain) (36º 55'-37º 15' N, 2º 31'-3º 40' W; maximum altitude 3482 m a.s.l.) ~50 small lakes of glacial origin lie at an elevation of ~2800–3100 m a.s.l. (Fig. 1). Their catchment basins consist of siliceous bedrock, mainly comprised of bare mica-schist with graphite and feldspar (Puga et al., 2007). Soil development is poor and the vegetation surrounding some of the lakes is restricted to sparse wet meadows (hygrophilous alpine tundra) (Fig. S1, Supplementary material). Thus, lake biogeochemistry and ecology is strongly influenced by external atmospheric inputs of elements such as Ca and P associated with massive depositions of dust from the Sahara Desert. The Sierra Nevada summit experiences a high-mountain, semi-arid

Mediterranean climate with a warm, dry season from ~June to October. The meteorological station at the summit (2507 m asl) reports a mean annual temperature of 3.9 ºC and total precipitation of 693 mm, with 80% falling as snow between October and April (Worldwide Bioclimatic Classification System 1996-2018). Above an altitude of 2500 m, approximately 95% of precipitation falls as snow. The lakes are typically ice-covered from November to June, but this can differ from year to year as a result of variations in annual climatic conditions (Barea-Arco et al., 2001; Morales-Baquero et al., 2006; Pérez-Martínez et al., 2007).

Six permanent lakes were strategically selected to be representative of the different lake types characterizing the Sierra Nevada Mountains using the following criteria: permanent lakes with maximum depth greater than 2.0 m and non-rocky bottoms (to ensure retrieval of a suitable sediment core for analyses), and lakes located in different valleys to represent the regional heterogeneity of lakes and valleys of the Sierra Nevada. The six lakes, Río Seco (RS), Río Seco Superior (RSS), Aguas Verdes (AV), Borreguil (BG), Mosca (MC), and Cuadrada (CD), are all located within an 8 km radius, and with the exception of MC, are located on the south face of the Sierra Nevada (Table S1, Supplementary material).

The lakes are typically shallow (maximum depth <5 m), small (surface area <1 ha), clear, and well-mixed (Table S1 and Fig. S1, Supplementary material). Given these characteristics, these lakes are largely littoral in nature and lack a clearly differentiated profundal zone. The lakes are circumneutral to slightly acidic, and are low in alkalinity and primary production (Table S1, Supplementary material). These shallow lakes are fishless and do not thermally stratify during the ice-free period.

CD and RSS lakes are currently closed basin systems and show little meadow development in their watersheds (Table S1 and Fig. S1, Supplementary material). The

186 remaining four lakes are open basin lakes that have surface inlets or outlets. Lakes CD,

187 RSS, RS and BG may decrease in water level during the summer, whereas AV and MC

188 do not usually show significant water-level reductions. However, the significance of the

189 water-level reductions in all six lakes is dependent on annual meteorological conditions.

190 As summer progresses, the meadows in the catchments can dry out (Fig. S2,

191 Supplementary material). There is currently minimal human activity around the lakes,

192 consisting mainly of mountaineers and restricted herding in some catchments.

193 Additional chemical and biological details concerning the study lakes can be

194 found elsewhere (Morales-Baquero et al., 1999; Morales-Baquero and Conde-Porcuna,

195 2000; Pérez-Martínez et al., 2007; Reche et al., 2001; Reche et al., 2005).

196 **2.2. Field sampling**

197 Sediment cores were taken from the deepest part of the lake by a slide-hammer

198 gravity corer (Aquatic Research Instruments, USA), with a 6.9 cm inner diameter

199 during the summer of 2011, with the exception of RS which was sampled in 2008. The

200 cores were sectioned on-site into 0.25 cm thick layers for the upper sections of the cores

201 and into 0.5 cm intervals for the remainder of the cores, with the exception of RS which

202 was sectioned at 0.5 cm contiguous intervals for the entire core length. The samples

203 were extruded into plastic zip-bags and stored in a ~4 °C refrigerator for later analysis.

204 On-site specific conductivity and pH measurements were conducted with a

205 multiparameter probe (Oakton PC300) following calibration for each lake. At each

206 coring site (i.e. the deepest part of the lake), tube samplers (6.7 cm diameter) of

207 different lengths were used to collect an integrated sample of the entire water column.

208 Water samples for the measurement of nutrient concentrations, alkalinity and calcium

209 were collected in acid-washed polyethylene bottles. Samples for dissolved organic

210 carbon (DOC) analysis were stored in pre-combusted amber glass bottles at

approximately 4ºC in the dark until analysis. Field samples were obtained following Pérez-Martínez et al. (2020).

Three representative sampling points in the wet meadows surrounding RS and MC were chosen for sampling epiphytic diatoms. Vegetation samples were taken at 0.5 m from the lake shore by cutting from their bases approximately five plant leaves with scissors and then amalgamating the sample. The samples were stored in glass containers and kept at 4º C, adding 1 mL of 50:50 mixture solution of H_2SO_4 and HNO_3 until further analysis.

2.3. Sediment chronology and laboratory analyses

Sediment cores were dated using gamma spectrometry (DSPec, Ortec®) techniques by measuring activities of radioisotopes (^{210}Pb, ^{137}Bi and ^{137}Cs) following the procedures outlined in Schelske et al. (1994) and Appleby & Oldfield (1978). Briefly, freeze dried sediment from a selection of 15-20 intervals from each core were weighed into plastic vials, sealed with two-ton epoxy, and allowed to sit for at least two weeks to ensure equilibrium between ^{226}Ra and ^{214}Bi prior to being placed into germanium gamma counters (Schelske et al., 1994). Sediment ages were estimated from unsupported ^{210}Pb activities using the constant rate of supply (CRS) model (Appleby and Oldfield, 1978).

Water chemistry variables were analyzed following the techniques detailed in APHA (1998) and in Pérez-Martínez et al. (2020). Total nitrogen (TN) and total phosphorus(TP) were measured as NO^{3-} by the ultraviolet method and as soluble reactive phosphorus, respectively. Dissolved silica (DSi) was analyzed by the molybdenum blue method. Dissolved calcium (Ca) concentrations were measured by atomic absorption and dissolved organic carbon (DOC) concentrations were determined by thermal oxidation following the method described by Mladenov et al. (2008). Total

235   alkalinity was measured by the acid titration method. For further details on sediment

236   chronology and laboratory analyses, see Jiménez et al. (2018).

237   **2.4. Diatom analysis**

238   Diatom samples from both the sediment core and wet meadow vegetation (epiphytic

239   diatoms) were processed closely following techniques described in Wilson et al. (1996).

240   In brief, diatom samples were prepared by digesting sediment samples with a 50:50

241   mixture solution of H_2SO_4 and HNO_3. The processed samples were allowed to settle

242   overnight, and the supernatant was then removed, and distilled water was added. This

243   procedure was repeated until the slurries reached a circumneutral pH. Slurries were then

244   strewn onto cover slips and mounted onto slides with Naphrax®. For each sample, a

245   minimum of 300 diatom valves were counted using a Leica microscope fitted with a

246   100X fluotar objective (N.A. = 1.4) and using differential interference contrast optics

247   under oil-immersion at 1000X magnification. Diatoms were identified to the species

248   level or lower using a selection of taxonomic sources, including Krammer and Lange-

249   Bertalot (1986–1991), Camburn and Charles (2000), Lange-Bertalot and Melzeltin

250   (1996), Hofmann et al. (2011), Van de Vijver et al (2002), Bey and Hector (2013) and

251   Lange-Bertalot et al. (2017). Diatom counts were expressed as a percent abundance

252   relative to the total number of diatom valves counted in each sedimentary interval.

253   **2.5. Climate data and Saharan deposition metrics**

254   We use MAAT Madrid (mean annual air temperature series from Madrid station, 1869–

255   2011) and AP San Fernando (annual precipitation series from San Fernando station,

256   1839-2011) as representative of air temperature and precipitation tendencies of the

257   greater Sierra Nevada region during the last 180 years. These two series strongly

258   correlate with shorter series of homogenized mean annual temperature and precipitation

259   records from stations close to the Sierra Nevada summits. For further details on climate

260   data, see Jiménez et al. (2018).

261   Sierra Nevada summits receive a high concentration of atmospheric dust

262   deposition annually because: 1) they are close to the Sahara Desert (70% of dust export

263   is deposited within the first 2000 km); 2) they are at high altitudes (the mainstream of

264   Saharan dust transport is between 1500 and 4000 m asl); and 3) they are in the path of

265   the Saharan dust particles' movement toward the western Mediterranean (Pey et al.,

266   2013). A clear summer prevalence of Saharan dust episodes is observed in the western

267   part of the Mediterranean (Pey et al., 2013) and specifically in the Sierra Nevada area

268   (Morales-Baquero et al., 2006; Morales-Baquero and Pérez-Martínez, 2016). Because

269   Sierra Nevada lakes have naturally low primary production and low cation

270   concentrations, we expect that the Ca and P-rich Saharan atmospheric deposition will

271   have an influence on primary producers (specifically diatoms), which are sensitive to

272   nutrient and ionic changes. To test this hypothesis, we used two indexes that are

273   representative of Saharan dust emissions: the wNAO (winter North Atlantic Oscillation)

274   index and the Sahel precipitation index (SPI). The intensity of Saharan dust emission

275   and transport has been linked to wNAO (Moulin et al., 1997) and to the Sahel drought

276   (Chiapello et al., 2005; Moulin and Chiapello, 2004). Both indexes are highly correlated

277   to sedimentary proxy records of Saharan dust deposition derived from RS Lake (Zr/Al

278   record) and from an ice core in the Alps (Ca record) (see Jiménez et al. (2018) for

279   further details on Saharan dust metrics).

280   **2.6. Data analyses**

281   Diatom zones were identified through cluster analysis using constrained incremental

282   sum of squares (CONISS), square root transformation of percentages data and chord

283   distance as the dissimilarity coefficient using the program Tilia Graph View (TGView),

284 version 2.1.1 (Grimm 2016), with the number of important zones determined by the

285 broken stick model (Bennett, 1996). CONISS analysis was performed on all diatom taxa

286 identified for each lake. For figure clarity, only the most common taxa are presented in

287 the species assemblages and several taxa were grouped into complexes if they shared

288 similar trends through time.

289   Detrended correspondence analysis (DCA) was applied to non-transformed

290 relative abundance data as a means to summarize the main variation in the diatom

291 assemblage data. DCA is a useful approach for detecting and summarizing the major

292 patterns of variation and for identifying the presence of any trends in a stratigraphical

293 sequence because sample scores can be scaled as standard deviation units of

294 compositional changed or turnover (Birks, 1998). Only taxa with relative abundance

295 >1% in at least one sediment sample interval were included in the ordination analysis.

296 DCA axis 1 (DCA 1) sample scores were used to statistically test the relationship

297 between diatom assemblages and climatic and atmospheric variables as predictor

298 variables in regression models (Birks, 1998, 2012). Ordination analyses were performed

299 using the vegan (Oksanen et al., 2015) package for the R software environment (R

300 Development Core Team, 2015).

301   To determine whether there were any significant relationships between climate

302 and dust metrics (MAAT Madrid, AP San Fernando, the wNAO index and the SPI) and

303 sedimentary proxies (relative abundance of individual diatom taxa for species-scale

304 trends, downcore DCA 1 scores for assemblage-scale trends), a Pearson correlation

305 analysis was applied using STATISTICA 7 program (Statsoft). The data were tested for

306 normality using the Kolmogorov Smirnov test prior the correlation analysis. The

307 annually resolved climate and dust metrics were averaged over the period of

accumulation for each dated interval, thereby integrating the instrumental data with the paleolimnological data (Sorvari et al., 2002).

To identify the explanatory variables of diatom assemblage changes as well as individual diatom species, model selection analyses (Burnham and Anderson, 2002) were performed with climate and atmospheric variables as independent variables, and diatom DCA 1 scores as the dependent variable using the MuMIn (Multi-Model Inference; Bartoń, 2014) package for the R software environment. Thus, the results of the regression indicate the drivers of the main shift in diatoms. To normalize the variance, explanatory variables, previously averaged over the period of accumulation for each dated interval, were z-score transformed prior to the analyses. Akaike's information criterion adjusted for sample size (AICc; Burnham and Anderson, 2002) was used to select the optimum model. Models with a difference of ΔAICc <2 compared to the lowest AICc were considered the best models and statistically equivalent. The significance and the percentage of variance explained for each variable was determined to define the contribution to the final model. Residuals of the final models were examined for normality and outliers were identified by using the outlier test function from car R package (Bonferroni Outlier Test). To avoid spurious relationships in multiple regression results, multicollinearity among the explanatory variables were explored by analyzing the variance inflation factors (VIFs). Breakpoint analyses using a two-segment piecewise linear regression were applied to MAAT Madrid and AP San Fernando series data to identify the timing of largest change (Toms and Lesperance, 2003).

3. Results

3.1. Geochronology

The unsupported ^{210}Pb inventory was contained within the upper 7-13 cm in the six sediment cores, reflecting the typically low rates of sediment accumulation in high altitude lakes (Moser et al., 2019). The average sedimentation rate value for the past ~50 years ranged from 0.01 to 0.03 g cm^{-2} year^{-1}, which corresponds to a temporal resolution between 2 and 5 years per interval in the sediment cores. The ^{210}Pb dates show a negative exponential curve in all the lakes with increasing associated errors from top to bottom. The decline in RSS and CD was more gradual than in the other lakes. The results of the ^{137}Cs activity are generally in good agreement with the ^{210}Pb dates. Analyses identified peaks in the ^{137}Cs activity which were coincident with the ^{210}Pb CRS (constant rate of supply) dates of 1960–1970 and consistent with the 1963 peak in atmospheric radioisotopic fallout. Further details and ^{210}Pb and ^{137}C activities as well as ^{210}Pb dates and associated errors estimated by the CRS model are given in Jiménez et al. (2018).

3.2. Climate data and Saharan deposition data

MAAT Madrid (mean annual air temperature series from Madrid station) show an increasing trend since the first decades of the 20th century, with steeper increases since the 1970s (Fig. 2). The breakpoint analyses identified a threshold change in the early 1970s (breakpoint = 1972 ± 4.7 years, p < .0001) whereas a potential additional breakpoint, not statistically significant, is also identified in the time interval of 1912–1915. Overall, AP San Fernando record shows than the precipitation was lower in the 20th century than in the second half of the 19th century. The last 40 years of the AP San Fernando record exhibit persistent low precipitation values that were particularly low from 1985 to 1995, when an acute period of drought occurred in Southern Spain (Udelhoven et al., 2009). No significant breakpoint was identified with the precipitation data. However, studies on Andalucía (the region in which Sierra Nevada is located)

16

highlight a general decreasing trend in the spring and annual precipitation series from the 1970s, with a period of marked drought in recent years (Castro-Díez et al., 2007) as the precipitation trend shows in our figure 2. As a result of increasing temperatures and decreasing precipitation since ~1970, the region likely experienced a warmer and drier ambient climate than in previous decades, with higher evaporation rates and less water availability.

SPI and the wNAO index can be considered as predictors of the transport and intensity of Saharan dust events in the Sierra Nevada and representative of P and Ca deposition trends in this area. Both indexes highly correlated with Zr/Al measured in RS sediment core (as an estimate of Saharan dust deposition in Sierra Nevada) and with a Saharan calcium series from an ice core obtained from a French Alps glacier (Jiménez et al., 2018). Both indexes experienced their lowest (SPI) and highest values (wNAO) in the past ~50 years (Fig. 2) indicating a period of the highest Saharan input. The most negative values (dry period) of the SPI record occurred from ~1970 to the 1980s onward, with the lowest values observed during the 1980s–1990s while the most positive values of wNAO index occurred during the 1980s–1990s (Fig. 2).

3.3. Trends in diatom assemblages

Epiphytic diatom assemblages (Table S2, Supplementary material) from the two representative meadow vegetation samples were dominated by species from the genera *Gomphonema, Pinnularia, Eunotia* and by *Nitzschia alpina* in RS and *Achnanthidium minutissimum, Encyonema minutum* and *Gomphonema spp.* in MC.

The diatom taxa identified in the six study lakes consisted almost totally of benthic species, with the exception of the habitually described as tychoplanktonic species *Tabellaria flocculosa* strain IV (*sensu* Koppen) and *Aulacoseira alpigena*. In all

17

of the study lakes, diatom assemblages were dominated by small benthic fragilarioid taxa such as *Staurosira venter* in RS, *Staurosirella pinnata* in AV and RSS, *Staurosira pseudoconstruens* in MC and *Pseudostaurosira brevistriata* in MC, BG and CD Lake (Fig. 3). Other diatom taxa with notable contributions to the assemblages include *A. alpigena* in RS, *A. minutissimum* in BG, and a variety of *Gomphonema* species in RS and BG. Two lakes had diatom assemblages that were dominated by one fragilarioid species (*P. brevistriata* in CD and *S. pinnata* in RSS) contributing more than 70% relative abundance for the entire ~180-year record.

In the six sediment core records, diatom assemblages show changes throughout time (Figs. 3 and 4), with larger changes occurring in RS, BG and CD than in AV and MC, and even more subtle changes in RSS. The greatest compositional change identified by CONISS and the broken stick analysis occurred during the 1960-80s in RS, BG, AV and MC, and at the turn of the 19th century in RSS and CD (Fig. 3).

Within the small Fragilariaceae group, an increase of *S. pinnata* in the last ~30 years is observed in AV, MC, whereas in RS and BG this taxon is a new arrival to the assemblage ~1970. Concurrent with the increase in *S. pinnata* is the arrival and increase in a variety of taxa that hitherto occurred in trace abundances including a variety of small-sized *Navicula* (*sensu-lato (s.l.)*), *Nitzschia* spp*., Cymbella (s.l), Amphora (s.l.),* and *Achnanthes (s.l)* taxa.

Overall, a shift from a variety of acidophilus taxa (*A. alpigena*, *T. flocculosa* strain IV*, C. lauta, Brachysira brebissonii, Frustulia crassinervia, and Psammothidium curtissimum*) to alkaliphilous species (*Navicula cryptocephala, N. cryptotenella, Nitzschia graciliformis, N. perminuta, N. alpina, Adlafia minuscula, Sellaphora pupula, Amphora copulata, A. pediculus*) (Rühland and Smol, 2002; Siver and Basquette, 2004;

405 Catalan et al., 2009; Falasco and Bona, 2011; Jacques et al., 2016) is observed in our set

406 of lakes (Fig. 3).

407 Of note is the decrease in the relative abundances of epiphytic and littoral taxa in

408 the more recent sediments of RS, BG, AV, and MC, such as *Gomphonema* spp.,

409 *Pinnularia* spp., *Eunotia* spp. and *A. minutissimum* (Fig. 3). This trend was particularly

410 evident in RS and BG, the two lakes with the highest meadows area and meadow/lake

411 area ratios. Moreover, a variety of taxa commonly associated with lower pH including

412 *Eunotia* spp., *T. flocculosa* strain IV, *Caloneis lauta, B. brebissonii, F. crassinervia*, and

413 *P. curtissimum* decreased in the upper intervals of the cores of RS, BG, AV, MC and

414 CD. This declining trend in epiphytic diatom taxa occurred at approximately the same

415 time (during the 1960s and 1980s) among RS, BG, AV and MC lakes, and ~1920 in

416 CD.

417 Apart from CD and RSS, all other lakes registered changes in the diatom record

418 between the 19th and 20th centuries, which are particularly notable in RS and BG where

419 CONISS identified a secondary zone. In contrast to the other 5 study lakes, RS diatom

420 assemblages include high relative abundances of the more heavily silicified and

421 tychoplanktonic *Aulacoseira alpigena*, which showed its highest relative abundances

422 during the second half of the 19th century and early 20th century (maximum relative

423 abundance of 44%). Thereafter there is a clear decline in this species to near

424 disappearance towards the top of the core. *Aulacoseira* taxa were also present in BG and

425 CD, although in considerably lower relative abundances. *A. alpigena* in BG shows a

426 similar trend to RS. In contrast to other lakes, *Aulacoseira* species in CD are present for

427 a brief period in the 19th century (maximum relative abundance of 7.6%) and disappear

428 at the turn of the 20th century concurrent with the main period of diatom assemblage

429 change identified for this lake (Figs. 3 and 4).

430   The total diatom assemblage variance captured by DCA 1 scores varied between

431   66% (RS) and 42% (CD). The overall diatom compositional changes are reflected by

432   the substantial changes in DCA 1 sample scores plotted against ^{210}Pb-estimated age

433   (Fig. 4). Major periods of diatom assemblage change indicated by trends in DCA 1

434   sample scores trends occurred between ~1960 and ~1980 in RS, BG, AV and MC lakes,

435   and at the turn of the 20th century in RSS and CD Lakes.

436   **3.4. Relationships between diatom data and instrumental records**

437   DCA 1 scores were correlated to air temperature in all the lakes (p<0.001) with the

438   exception of RSS, which showed minimal change in diatoms over time (Fig 3).

439   Moreover, DCA 1 scores are correlated with SPI in RS, BG and MC (all p<0.01) and

440   with precipitation in RS and BG (p<0.01).

441   All the explanatory variables included in model selection analyses yielded VIFs

442   <5 and therefore were kept in the analysis due to the low degree of collinearity. The

443   model selection analysis (Table 1) indicate temperature to be the main predictor variable

444   of DCA 1 scores (i.e. the main direction of diatom assemblage changes) for all the study

445   lakes except for RSS. Secondary explanatory variables of DCA 1 scores are SPI (RS

446   and BG) and wNAO (MC). The amount of variance explained by these variables ranged

447   from 61% in CD to 91% in RS. A null model was obtained for DCA 1 scores in RSS.

448   In addition to assemblage-scale analysis, we also performed model selection

449   analysis on individual diatom species that were selected as being representative of the

450   main diatom shifts in the study lakes, including *S. pinnata* and *A. alpigena*. The main

451   predictor variable for changes in *S. pinnata* relative abundance in RS, AV, BG and MC

452   is temperature with SPI, wNAO and AP San Fernando as secondary explanatory

453   variables. All models explained >60% of the observed variation (Table 2). AP San

454   Fernando is the main predictor variable of *S. pinnata* relative abundance in RSS but the

455 model explained <15% of the observed variation. The main predictor of *A. alpigena*

456 relative abundance in RS is temperature and secondarily AP San Fernando (Table 2).

3.5. Relationships between diatom data and other biological proxies

458 For graphical and comparison purposes, we use the Cladocera PCA scores and the

459 Chlorophyll-*a* values obtained in Jiménez et al. (2018). The diatom DCA scores,

460 Cladocera PCA scores and Chl-*a* values for the six study lakes are shown in

461 supplementary figure S3 to allow the comparison of the timing of main changes in

462 biological proxies across the lakes. The main changes in sedimentary Chl-*a* occur

463 simultaneously, with a significant increase in all six lakes between ~1960 and ~1970.

464 This change is roughly coincident with the main change in diatom assemblages in RS,

465 AV, MC and BG, whereas the main change in diatoms occurs earlier in RSS and CD

466 (Fig. S3). Regarding subfossil Cladocera, their main change is observed during the late-

467 1980s and during the 1990s across the lakes.

4. Discussion

469 Recent changes in climate and Saharan dust deposition had important influences on

470 diatom assemblages in Sierra Nevada lakes. Air temperature was determined to be the

471 strongest predictor variable for diatom compositional changes in all of our study lakes,

472 with the exception of RSS. Changes in precipitation were also important, although to a

473 lesser degree. However, the combination of increasing temperature and decreasing

474 precipitation led to a drier environment with higher evaporation rates and less water

475 availability. It is not surprising, therefore, that the largest diatom compositional changes

476 occurred during periods of accelerated temperature increase and declines in

477 precipitation. For example, in four study lakes, the diatom shifts between the 1970s and

478 1980s were concurrent with the steep rise in regional air temperature and with the

479 decrease in precipitation over the past few decades. In the other two lakes (CD and

480   RSS), the largest diatom compositional change corresponded to an initial rise in

481   regional air temperature in the early 20th century. The warming trend starting in the

482   early 20th century is also a period of relatively low precipitation that followed a wet

483   period at the end of the 19th century (Fig. 2). In conjunction with a warmer and drier

484   climate, diatoms were also responding to recent increases in Saharan atmospheric

485   deposition (Fig. 2) because of the intensification of atmospheric input since ~1980

486   onward. The two proxies for atmospheric Saharan deposition (wNAO index and SPI)

487   were important predictor variables of the diatom assemblage changes in several lakes

488   (Table 1).

489   The strong representation of small, benthic, fragilarioid taxa (S. *brevistriata, S.*

490   *venter, S. pinnata, S. pseudoconstruens*) in all six sites reflects the relatively cold

491   environmental conditions and short growing seasons of these shallow, high altitude

492   lakes (Karst-Riddoch et al. 2009). These fast-growing, generalist taxa are widespread

493   and commonly dominate cold, alkaline to circumneutral, oligotrophic Arctic and alpine

494   lakes and ponds (Rühland and Smol, 2002; Michelutti et al., 2007; Keatley et al. 2008;

495   Lotter et al., 2010; Rühland et al., 2015). They are amongst the first to colonize lakes

496   and ponds following deglaciation and ice off because they are able to flourish in these

497   relatively harsh conditions (Griffiths et al., 2017).

498   Despite the prominence of fragilarioid taxa throughout the sedimentary records,

499   there were clear changes in diatom assemblage composition in our study lakes. For

500   example, the shift in dominance from epipelic *Staurosira venter* and epiphytic

501   *Gomphonema* spp. to tychoplanktonic *Aulacoseira alpigena* in RS during the latter part

502   of the 19th century is coincident with a wet and cold period at this time in the Sierra

503   Nevada. Changes in *Aulacoseira* taxa were also observed in BG and CD, although less

504   pronounced than in RS. Although all of these lakes are quite shallow (<5.0 m), changing

climatic conditions may have provided a favourable environment for this heavily

silicified diatom. Namely, it is plausible that during this wet and cold period, water

inflow to the lake increased, and water turbulence was strong enough to allow these

heavier diatoms to maintain a planktonic existence (Kilham et al., 1996; Round et al.,

1990) despite the relatively shallow water column. The decline in *Aulacoseira* taxa

(particularly in RS) starting ~1920, with further declines following the ~1960s, were

consistent with the onset of warmer and drier conditions (Fig. 2). In the Sierra Nevada

region, a drier and warmer climate led to a reduction of snow (Bonet et al., 2016),

reduced inflows to the lakes, lower water levels, and thus probably reduced lake water

turbulence, all of which would hinder *A. alpigena* growth. The reduction of *Aulacoseira*

species to trace abundances in CD occurred earlier, concurrent with the start of the drier

and warmer period during the early-20th century. The earlier response in this lake may

be related to it being 140 to 210 m lower in elevation than the other lakes located on the

south face of Sierra Nevada and 80 m lower than MC, the only lake located at the north

face and to its location in the western-most part of Sierra Nevada Mountains, where

precipitation declines are the greatest (Pérez-Luque et al., 2016). Given the

physioecological characteristics of *A. alpigena*, it is not surprising that air temperature

and precipitation were identified as explanatory variables for variations in *A. alpigena*

relative abundance in RS (Table 2)..

A shift from a suite of acidophilus taxa (*A. alpigena*, *T. flocculosa* strain IV*, C.*

lauta, B. brebissonii, F. crassinervia, and P. curtissimum) to an assemblage of

alkaliphilous taxa (*N. cryptocephala, N. cryptotenella, N. graciliformis, N. perminuta*,

N. alpina, *A. minuscula*, *S. pupula*, *A. copulata*, *A. pediculus*) in the post-~1960s

sediments indicates an increase in ionic composition and an alkalinization trend in our

Sierra Nevada lakes. The combination of warmer temperatures, lower precipitation and

increased dust input likely explain the increase in alkalinity in our naturally softwater lakes that our diatom records indicate. Warming and a longer ice-free period can increase solute concentration through evapoconcentration and longer exposure to Saharan Ca inputs..

S. pinnata shows an increasing trend (often occurring for the first time above trace abundances) during warmer, drier and dust input increasing periods since the ~1970s in four of the five Sierra Nevada lakes where this taxon occurs in the sedimentary record. Consistently, temperature, SPI and wNAO were identified as the main predictor variables of *S. pinnata* abundances in our study lakes (Table 2). The increase of *S. pinnata* may be the result of the increased alkalinity caused by evapoconcentration plus Saharan dust. Catalan et al. (2009) and Weckström et al. (1997) also associated *S. pinnata* with higher levels of alkalinity than *S. venter* and *S. construens* in high altitude and latitude lakes, respectively. In agreement with a rise in *Daphnia* with Ca enrichment of Sierra Nevada lakes reported by Jiménez et al. (2018), our diatom results are indicative of recent alkalinization of these same lakes that can be linked to increases in Ca-rich Saharan dust inputs and evapoconcentration since the 1970s.

Our diatom records also appear to be tracking the development of catchment wetland plants from the beginning of the 20th century until the ~1970s. For example, in lakes surrounded by meadows, increases in epiphytic, bog-inhabiting species such as *Gomphonema* spp. (Table S2, Michelutti et al., 2006; Vinocur & Maidana, 2010), *Pinnularia* spp. (Table S2, Michelutti et al., 2006; Paull et al., 2017; Vinocur & Maidana, 2010), *Eunotia* spp. (Table S2; Falasco and Bona, 2011; Küttim et al., 2017) and *A. minutissimum* (Table 1,Keatley et al., 2006; Lotter et al., 2010) were observed during this period in lakes. Following the 1960s, these taxa markedly declined, as the

555 steep rise in temperature and decrease in precipitation would have resulted in a drier

556 catchment, with less water availability for plant growth and increasing drought.

557   The presence and extension of meadows determines the presence in sediment

558 cores of diatom epiphytic species, presumably the more meadow-extension/lake-area

559 extension the more significance of diatom epiphytic in sediments. Our diatom

560 assemblages agree with this premise, being the presence of epiphytic species much

561 higher in open basin lakes with meadows than in closed basin lakes with no or reduced

562 meadow extension (Fig. 3 and Fig. S1, Supplementary material). In our study, the

563 changes in periphytic diatom abundances are more conspicuous in BG and RS than in

564 AV and MC, likely because the latter two lakes drain smaller meadow areas (Figure S1,

565 Supplementary material) and because they are located close to habitually permanent

566 snow patches providing water to their catchments. These features would explain the

567 higher gradient length of DCA 1 in BG and RS than in AV and MC. However, the most

568 notable difference is the main period of diatom change among lakes, which occurs

569 between ~1960 and ~1980 in all lakes, with the exception of RSS and CD in which it is

570 observed at the turn of the 20th century. As we have already discussed, the lower

571 elevation of CD and its westernmost location may explain the earlier response of CD to

572 warming. In RSS, diatom assemblage change is much less conspicuous and show a

573 significantly shorter DCA gradient lenght than in the other five studied lakes despite it

574 recording noticeable changes in chlorophyll-*a* and in cladoceran assemblages over the

575 last few decades (Figure S3, Supplementary material). This fact probably suggests that

576 diatoms respond to other drivers than those mainly influencing overall algal production

577 and cladoceran assemblages. RSS is a closed basin lake with the smallest lake surface

578 area and the steepest bathymetric slopes, which probably resulted in a low niche

579 differentiation for diatoms. Therefore, it is not surprising that this lake shows the lowest

25

species diversity and is dominated by generalist and pioneering species such as *S. pinnata* (Lotter and Bigler, 2000; Summers et al., 2017) throughout the core. Previous studies in Sierra Nevada lakes have also shown the relationship of catchment and lake morphometry and location with chemical characteristics of lakes (Morales et al., 1999; 2006) and with the zooplankton composition and abundance (Morales-Baquero et al., 2019; Pérez-Martínez et al., 2020).

Similar to our diatom findings, increases in both regional air temperature and Saharan dust deposition were also the best predictors of subfossil cladoceran assemblage changes and of increases in sedimentary chlorophyll-*a* examined in the same six lakes (Jiménez et al., 2018). The increasing trend in chlorophyll-*a* starting ~1970 across the lakes could be partially attributed to Saharan P input together with climate-related factors such as temperature increase, precipitation decrease and lengthening of the ice-free period. All algal groups may have been favoured by P input, but presumably planktonic species could be more favoured than benthic ones since the latter have access to sediment nutrient (Vadeboncoeur et al. 2003, 2014; Godwin et al. 2014). However, we did not observe diatom assemblage changes in our study lakes that might be attributed to a nutrient increase, but rather to changes mainly governed by alkalinity and water turbulence. It is possible that the strong sensitivity of diatoms to acid-base gradients outweigh the effect of nutrients (Rivera-Rondón & Catalan, 2019). It may also be that the dominance of benthic and periphytic diatom species, which have access to sediment nutrients and are not so limited by nutrient concentration (Vadeboncoeur et al. 2003), weaken the nutrient increase effect. Thus, the effect of Saharan input differs among proxies, with P input significantly affecting trends in Chl-*a*, whereas Ca input appears to be more significant for diatom assemblage changes (via lake water alkalinization) and *Daphnia* spp. by direct water Ca absorption.

605   Likewise, changes in cladoceran assemblages during the 1990s lag shifts in

606   diatom assemblages by about two decades, in spite of the observation that the temporal

607   changes of both taxonomic groups can mainly be explained by climate variables.

608   Climate change causes a wide range of lake physical and chemical responses (Adrian et

609   al., 2009; Rühland et al., 2015) and different group of organisms can respond to

610   different effects. In Sierra Nevada, diatoms mainly respond to acid-base gradient, water

611   column turbulence and catchment water availability, whereas the main cladoceran

612   assemblage change (a shift from *Chydorus sphaericus* to *Alona quadrangularis*)

613   beginning in the early 1990s was associated to longer ice-free period, increasing water

614   residence time and warmer waters (Jiménez et al., 2018). An amplification of these

615   climate effects linked to drought intensification beginning in the late-1980s likely

616   triggered the cladoceran species shift. It appears that different taxonomic groups may

617   respond to different climate-derived effects and have different thresholds of response.

618   Although each proxy responded to a particular climate-related effect, the nature of the

619   lake changes are rather similar, with changes in the three proxies suggesting longer ice-

620   free periods and less water availability in the area which was driven by both temperature

621   and precipitation (this study and Jiménez et al., 2018, 2019).

622   **6. Conclusions**

623   We assessed the long-term limnological effects of changes in climate and

624   Saharan dust deposition on Sierra Nevada summit ecosystems by analyzing changes in

625   diatom assemblages. Overall, our current diatom study provides new information on

626   changes in chemical and physical features of the lakes. The observed changes in

627   diatoms show that ecological shifts have occurred in shallow Sierra Nevada lakes,

628   starting at the turn of the 20th century and were especially evident during the latter half

629   of the 20th century. In particular, we conclude that Sierra Nevada lakes have

630 experienced lake alkalinization from Saharan dust input in combination with processes

631 related to a warmer and drier climate such as a reduction in lake water level and reduced

632 water turbulence as water inflows diminished. Diatom assemblage changes also indicate

633 an increasing aridity in lake catchment meadows since the 1960s. The increased aridity

634 of the Sierra Nevada is worrisome, as this region provides a variety of ecosystem

635 services (Palomo et al., 2013). Differences in lake position, morphometry and

636 catchment features (such as the presence of meadows) can explain differences in the

637 timing and magnitudeof the ecological responses we recorded among lakes Moreover,

638 diatom assemblages seem to respond to different atmospheric and climate-related

639 effects than cladoceran assemblages and Chl a concentrations, which were previously

640 analyzed in the same set of lakes.

641   The possible alkalinization of lentic aquatic systems as a results of climate

642 change and atmospheric deposition likely occurs in other areas and, particularly in arid

643 and semiarid areas influenced by dust inputs. The fact that such areas are present

644 throughout the world (Ginoux et al., 2012), containing numerous mountainous aquatic

645 systems, indicates that more research in this area is warranted.

646

656

657

658

659

660 **References**

661 Adrian, R., O'Reilly, C. M., Zagarese, H., Baines, S. B., Hessen, D. O., Keller,W., . . .

662   and Winder, M. (2009). Lakes as sentinels of climate change. Limnology and

663   Oceanography, 54, 2283–2297.

664 APHA, American Public Health Association (1998). Standard methods for the

665   examination of water and wastewater. American Public Health Association,

666   American Water Works Association, and Water Environment Federation,

667   Washington DC.

668 Appleby, P. G., & Oldfield, F. (1978). The calculation of lead-210 dates assuming a

669   constant rate of supply of unsupported ^{210}Pb to the sediment. Catena, 5, 1-8.

670 Barea-Arco, J., Pérez-Martínez, C., & Morales-Baquero, R. (2001). Evidence of a

671   mutualistic relationship between an algal epibiont and its host, *Daphnia pulicaria*.

672   Limnology and Oceanography, 46, 871-881.

673 Bartoń, K. (2014). MuMIn: Multi-model inference. R package version 1.10.0. Retrieved

674   from http://CRAN.R-project.org/package=MuMIn.

675 Battarbee, R., Charles, D., Bigler, C., Cumming, B., & Renberg, I. (2010). Diatoms as

676   indicators of surface-water acidity, in: Smol, J., & Stoermer, E. (Eds.), The

677   Diatoms: Applications for the Environmental and Earth Sciences. Cambridge,

678   Cambridge University Press, pp. 98-121. doi:10.1017/CBO9780511763175.007

679 Beniston, M. (2003). Climatic change in mountain regions: a review of possible

680   impacts. In Climate variability and change in high elevation regions: Past, present

681   & future (pp. 5-31). Springer, Dordrecht.

682 Bennett, K. D. (1996). Determination of the number of zones in a biostratigraphical

683   sequence. New Phytologist, 132, 155–170.

684   Bey M.-Y., & Ector, L. (2013). Atlas des diatomées des cours d'eau de la région Rhône-

685   Alpes. Tome 1 Centriques, Monoraphidées. Tome 2 Araphidées,

686   Brachyraphidées. Tome 3 Naviculacées: Naviculoidées. Tome 4 Naviculacées:

687   Naviculoidées. Tome 5 Naviculacées: Cymbelloidées, Gomphonématoidées.

688   Tome 6 Bacillariacées, Rhopalodiacées, Surirellacées. Direction régionale de

689   l'Environnement, de l'Aménagement et du Logement Rhône-Alpes, Lyon, 1182 +

690   27 pp., ISBN 978-2-11-129817-0.

691   Birks, H. J. B. (1998) Numerical tools in palaeolimnology –progress, potentialities, and

692   problems. Journal of Paleolimnology, 20, 307–332.

693   Birks, H. J. B (2012). Analysis of Stratigraphical Data, In: Birks, H. J. B., Lotter, A. F.,

694   Juggins, S., & Smol, J. P. (Eds.). (2012). Tracking environmental change using

695   lake sediments: data handling and numerical techniques (Vol. 5). Kluwer

696   Academic Publishers, Dordrecht, pp. 355-378.

697   Blanca, G., Cueto, M., Martínez-Lirola, M. J., & Molero-Mesa, J. (1998). Threatened

698   vascular flora of Sierra Nevada (southern Spain). Biological Conservation, 85,

699   269-285.

700   Blanco-Pastor, J. L., Fernández‑Mazuecos, M., & Vargas, P. (2013). Past and future

701   demographic dynamics of alpine species: limited genetic consequences despite

702   dramatic range contraction in a plant from the Spanish Sierra Nevada. Molecular

703   Ecology, 22, 4177-4195.

704   Bonet, F. J., Pérez-Luque, A. J., & Pérez-Pérez, R. (2016). 2.4. Trend analysis (2000-

705   2014) of the snow cover by satellite (MODIS sensor), in: Zamora Rodríguez, R.

706   J., Pérez Luque, A. J., Bonet, F. J., Barea-Azcón, J. M., & Aspizúa, R. (Eds.),

707   Impacts of Global Change in Sierra Nevada: Challenges for conservation, pp. 43.

708   Burnham, K. P., & Anderson, D. R. (2002). Model selection and multimodel inference:

709   A practical information-theoretic approach. New York, NY, USA: Springer-

710   Verlag

711   Camarero, L., & Catalan, J. (2012). Atmospheric phosphorus deposition may cause

712   lakes to revert from phosphorus limitation back to nitrogen limitation. Nature

713   Communications, 3, 1118.

714   Camburn, K.E., & Charles, D. F. (2000). Diatoms of low alkalinity lakes in the

715   northeastern United States. The Academy of Natural Sciences, Philadelphia,

716   Scientific Publication, 18, 152 pp.

717   Castro-Díez, Y., Esteban-Parra, M. J., Staudt, M., & Gámiz-Fortis, S. (2007). Cambios

718   Climáticos Observados en la Temperatura y la Precipitación en Andalucía en el

719   Contexto de la Península Ibérica y Hemisférico. Climate change in Andalusia:

720   trends and environmental consequences, 57-77.

721   Catalan, J., Barbieri, M. G., Bartumeus, F., Bitusik, P., Botev, I., Brancelj, A., . . .

722   Ventura, M. (2009). Ecological thresholds in European alpine lakes. Freshwater

723   Biology, 54, 2494–2517.

724   Chiapello, I., Moulin, C., & Prospero, J. M. (2005). Understanding the long-term

725   variability of African dust transport across the Atlantic as recorded in both

726   Barbados surface concentrations and large-scale Total Ozone Mapping

727   Spectrometer (TOMS) optical thickness. Journal of Geophysical Research:

728   Atmospheres, 110 (D18).

729   Falasco, E., & Bona, F. (2011). Diatom community biodiversity in an Alpine protected

730   area: a study in the Maritime Alps Natural Park. Journal of Limnology, 70, 157-

731   167.

732

Gallisai, R., Peters, F., Volpe, G., Basart, S., & Baldasano, J. M. (2014). Saharan dust deposition may affect phytoplankton growth in the Mediterranean Sea at ecological time scales. PloS ONE, 9, e110762.

García-Jurado, F., Jiménez-Gómez, F., & Guerrero, F. (2011). Effects of a dry period on the limnological characteristics of a Mediterranean high mountain lake. Limnetica, 30, 0005-16.

Ginoux, P., Prospero, J. M., Gill, T. E., Hsu, N. C., & Zhao, M. (2012). Global-scale attribution of anthropogenic and natural dust sources and their emission rates based on MODIS Deep Blue aerosol products. Reviews of Geophysics, 50. https://doi.org/10.1029/2012RG000388

Gobiet, A., Kotlarski, S., Beniston, M., Heinrich, G., Rajczak, J., & Stoffel, M. (2014). 21st century climate change in the European Alps—a review. Science of the Total Environment, 493, 1138-1151.

Godwin, S. C., Jones, S. E., Weidel, B. C., & Solomon, C. T. (2014). Dissolved organic carbon concentration controls benthic primary production: Results from in situ chambers in north-temperate lakes. Limnology and Oceanography, 59, 2112-2120.

González-Olalla, J. M., Medina-Sánchez, J. M., Lozano, I. L., Villar-Argaiz, M., & Carrillo, P. (2018). Climate-driven shifts in algal-bacterial interaction of high-mountain lakes in two years spanning a decade. Scientific Reports, 8.

Grabherr, G., Gottfried, M., Gruber, A., & Pauli, H. (1995). Patterns and current changes in alpine plant diversity. In Arctic and alpine biodiversity: patterns, causes and ecosystem consequences (pp. 167-181). Springer, Berlin, Heidelberg.

756   Griffiths, K., Michelutti, N., Sugar, M., Douglas, M. S., & Smol, J. P. (2017). Ice-cover

757   is the principal driver of ecological change in High Arctic lakes and ponds. PloS

758   ONE, 12, e0172989.

759   Grimm, E. C. (2016). Tilia y TGView 2.1.1 Illinois State Museum. Research and

760   Collection Center. Springfield, Illinois.

761   Hofmann, G., Werum, M., & Lange-Bertalot, H. (2011). Diatomeen im Süβwasser-

762   Benthos von Mitteleuropa. Bestimmungsflora Kieselalgen für die ökologische

763   Praxis. Über 700 der häufigsten Arten und ihre Ökologie. Ruggell, A.R.G.

764   Gantner Verlag, 908 p.

765   Jacques, O., Bouchard, F., MacDonald, L. A., Hall, R. I., Wolfe, B. B., & Pienitz, R.

766   (2016). Distribution and diversity of diatom assemblages in surficial sediments of

767   shallow lakes in Wapusk National Park (Manitoba, Canada) region of the Hudson

768   Bay Lowlands. Ecology and Evolution, 6, 4526-4540.

769   Jiménez, L., Conde-Porcuna, J. M., García-Alix, A., Toney, J. L., Anderson, R. S.,

770   Heiri, O., & Pérez-Martínez, C. (2019). Ecosystem Responses to Climate-Related

771   Changes in a Mediterranean Alpine Environment Over the Last~ 180 Years.

772   Ecosystems, 22, 563-577.

773   Jiménez, L., Romero-Viana, L., Conde-Porcuna, J. M., & Pérez-Martínez, C. (2015).

774   Sedimentary photosynthetic pigments as indicators of climate and watershed

775   perturbations in an alpine lake in southern Spain. Limnetica, 34, 439-454.

776   Jiménez, L., Rühland, K. M., Jeziorski, A., Smol, J. P., & Pérez-Martínez, C. (2018).

777   Climate change and Saharan dust drive recent cladoceran and primary production

778   changes in remote alpine lakes of Sierra Nevada, Spain. Global Change Biology,

779   24, e139-e158. doi: 10.1111/gcb.13878

780 Jiménez-Espejo, F. J., García-Alix, A., Jiménez-Moreno, G., Rodrigo-Gámiz, M.,

781   Anderson, R. S., Rodríguez-Tovar, F. J., ... & Pardo-Igúzquiza, E. (2014).

782   Saharan aeolian input and effective humidity variations over Western Europe

783   during the Holocene from a high altitude record. Chemical Geology, 374, 1-12.

784 Karst-Riddoch, T. L., Malmquist, H. J., & Smol, J. P. (2009). Relationships between

785   freshwater sedimentary diatoms and environmental variables in Subarctic

786   Icelandic lakes. Fundamental and Applied Limnology/Archiv für Hydrobiologie,

787   175(1), 1-28.

788 Keatley, B. E., Douglas, M. S. V., & Smol, J. P. (2006). Early-20th century

789   environmental changes inferred using subfossil diatoms from a small pond on

790   Melville Island, N.W.T., Canadian High Arctic. Hydrobiologia, 553, 15–26.

791 Keatley, B. E., Douglas, M. S., & Smol, J. P. (2008). Prolonged ice cover dampens

792   diatom community responses to recent climatic change in High Arctic lakes.

793   Arctic, Antarctic, and Alpine Research, 40, 364-372.

794 Kilham, S. S., Theriot, E. C., & Fritz, S. C. (1996). Linking planktonic diatoms and

795   climate change in the large lakes of the Yellowstone ecosystem using resource

796   theory. Limnology and Oceanography, 41, 1052-1062.

797   doi:10.4319/lo.1996.41.5.1052

798 Krammer, K., & Lange-Bertalot, H. (1986–1991). Bacillariophyceae, in: Ettl, H.,

799   Gerloff, J., Heynig, H., & Mollenhauer, D. (Eds.), Süßwasserflora von

800   Mitteleuropa, vol. 2 (1–4). Gustav Fischer Verlag, Stuttgart/Jena.

801 Küttim, L., Küttim, M., Puusepp, L., & Sugita, S. (2017). The effects of ecotope,

802   microtopography and environmental variables on diatom assemblages in

803   hemiboreal bogs in Northern Europe. Hydrobiologia, 792, 137-149.

804   Lange-Bertalot, H., & Metzeltin, D. (1996). Indicators of oligotrophy - 800 taxa

805   representative of three ecologically distinct lake types, Carbonate buffered -

806   Oligodystrophic - Weakly buffered soft water, in: Lange-Bertalot, H. (Ed.),

807   Iconographia Diatomologica. Annotated Diatom Micrographs. Vol. 2. Ecology,

808   Diversity, Taxonomy. Koeltz Scientific Books. Königstein, Germany, 2, 390 pp.

809   Lange-Bertalot, H., Hofmann, G., Werum, M., & Cantonati, M. (2017). Freshwater

810   benthic diatoms of Central Europe: over 800 common species used in ecological

811   assessment (p. 942). M. G. Kelly (Ed.). Schmitten-Oberreifenberg: Koeltz

812   Botanical Books.

813   Lequy, E., Conil, S., & Turpault, M. P. (2012). Impacts of Aeolian dust deposition on

814   European forest sustainability: a review. Forest Ecology and Management, 267,

815   240-252.

816   Lionello, P. (Ed.). (2012). The climate of the Mediterranean region: From the past to the

817   future. Elsevier.

818   Lotter A. F., Pienitz, R., & Schmidt, R. (2010). Diatoms as indicators of environmental

819   change in subarctic and alpine regions, in: Smol, J. P., & Stoermer, E. F. (Eds.),

820   The Diatoms: Applications for the Environmental and Earth Sciences, 2nd edition.

821   Cambridge: Cambridge University Press, 667 pp.

822   Lotter, A. F., & Bigler, C. (2000). Do diatoms in the Swiss Alps reflect the length of

823   ice-cover? Aquatic Sciences, 62, 125-141.

824   Loÿe-Pilot, M. D., Martin, J. M., & Morelli, J. (1986). Influence of Saharan dust on the

825   rain acidity and atmospheric input to the Mediterranean. Nature, 321(6068), 427-

826   428.

827   Magnani, A., Viglietti, D., Godone, D., Williams, M. W., Balestrini, R., & Freppaz, M.

828   (2017). Interannual variability of soil N and C forms in response to snow—cover

829   duration and pedoclimatic conditions in alpine tundra, northwest Italy. Arctic,

830   Antarctic, and Alpine Research, 49(2), 227-242.

831   Marañón, E., Fernández, A., Mourino-Carballido, B., MartÍnez-GarcÍa, S., Teira, E.,

832   Cermeno, P., ... & Morán, X. A. G. (2010). Degree of oligotrophy controls the

833   response of microbial plankton to Saharan dust. Limnology and Oceanography,

834   55(6), 2339-2352. doi:10.4319/lo.2010.55.6.2339

835   Michelutti, N., Douglas, M. S., Wolfe, A. P., & Smol, J. P. (2006). Heightened

836   sensitivity of a poorly buffered high arctic lake to late-Holocene climatic change.

837   Quaternary Research, 65, 421-430.

838   Michelutti, N., Wolfe, A. P., Briner, J. P., & Miller, G. H. (2007). Climatically

839   controlled chemical and biological development in Arctic lakes. Journal of

840   Geophysical   Research: Biogeosciences,   112(G3)

841   https://doi.org/10.1029/2006JG000396

842   Mladenov, N., Pulido-Villena, E., Morales-Baquero, R., Ortega-Retuerta, E.,

843   Sommaruga, R., & Reche, I. (2008). Spatiotemporal drivers of dissolved organic

844   matter in high alpine lakes: Role of Saharan dust inputs and bacterial activity.

845   Journal of Geophysical Research: Biogeosciences, 113(G2).

846   Mladenov, N., Sommaruga, R., Morales-Baquero, R., Laurion, I., Camarero, L.,

847   Diéguez, M. C., ... & Reche, I. (2011). Dust inputs and bacteria influence

848   dissolved organic matter in clear alpine lakes. Nature Communications, 2(1), 1-7.

849   Morales-Baquero, R., & Conde-Porcuna, J. M. (2000). Effect of the catchment areas on

850   the abundance of zooplankters in high mountain lakes. Verhandlungen der

851 Internationale Vereinigung für theoretische und angewandte Limnologie, 27,

852 1804-1808.

853 Morales-Baquero, R., & Pérez-Martínez, C. (2016). Saharan versus local influence on

854 atmospheric aerosol deposition in the southern Iberian Peninsula: Significance for

855 N and P inputs. Global Biogeochemical Cycles, 30(3), 501-513.

856 Morales-Baquero, R., Carrillo, P., Barea-Arco, J., Pérez Martínez, C., & Villar-Argaiz,

857 M. (2006). Climate-driven changes on phytoplankton–zooplankton coupling and

858 nutrient availability in high mountain lakes of Southern Europe. Freshwater

859 Biology, 51, 989-998.

860 Morales-Baquero, R., Carrillo, P., Reche, I., & Sánchez-Castillo, P. (1999). Nitrogen-

861 phosphorus relationship in high mountain lakes: effects of the size of catchment

862 basins. Canadian Journal of Fisheries and Aquatic Sciences, 56(10), 1809-1817.

863 Morales-Baquero, R., Pulido-Villena, E., & Reche, I. (2013). Chemical signature of

864 Saharan dust on dry and wet atmospheric deposition in the south-western

865 Mediterranean region. Tellus, Series B: Chemical and Physical Meteorology, 65,

866 18720.

867 Morales-Baquero, R., Pérez-Martínez, C., Ramos-Rodríguez, E., Sánchez-Castillo, P.,

868 Villar-Argaiz, M., & Conde-Porcuna, J. M. (2019). Zooplankton advective losses

869 may affect chlorophyll-a concentrations in fishless high-mountain lakes.

870 Limnetica, 38, 55-65.

871 Moser, K.A., Baron, J. S., Brahney, J., Oleksy, I., Saros, J.E., Hundey, E.J., Sadro, S.A.,

872 Kopáček, J., Sommaruga, R., Kainz, M.J., Strecker, A.L., Chandra, S., Walters,

873 D.M., Preston, D.L., Michelutti, N., Lepori, F., Spaulding, S.A., Christianson, K.,

874 Melack, J.M., & Smol, J.P. (2019). Mountain lakes: Eyes on global

875 environmental change. Global and Planetary Change, 178, 77-95.

876 https://doi.org/10.1016/j.gloplacha.2019.04.001

877 Moulin, C., & Chiapello, I. (2004). Evidence of the control of summer atmospheric

878 transport of African dust over the Atlantic by Sahel sources from TOMS

879 satellites (1979–2000). Geophysical Research Letters, 31(2).

880 doi: 10.1029/2003GL018931

881 Moulin, C., Lambert, C. E., Dulac, F., & Dayan, U. (1997). Control of atmospheric

882 export of dust from North Africa by the North Atlantic Oscillation. Nature, 387

883 (6634), 691-694.

884 Moulin, C., & Chiapello, I. (2006). Impact of human-induced desertification on the

885 intensification of Sahel dust emission and export over the last decades.

886 Geophysical Research Letters, 33(18), L18808,

887 doi:10.1029/2006GL025923Mulitza, S., Heslop, D., Pittauerova, D., Fischer, H.

888 W., Meyer, I., Stuut, J. B., ... & Schulz, M. (2010). Increase in African dust flux at

889 the onset of commercial agriculture in the Sahel region. Nature, 466(7303), 226.

890 Myers, N., Mittermeier, R. A., Mittermeier, C. G., Da Fonseca, G. A., & Kent, J.

891 (2000). Biodiversity hotspots for conservation priorities. Nature, 403, 853.

892 Nogués-Bravo, D., Araújo, M. B., Lasanta, T., & Moreno, J. I. L. (2008). Climate

893 change in Mediterranean mountains during the 21st century. AMBIO: A Journal

894 of the Human Environment, 37(4), 280-285.

895 Nogués-Bravo, D., López-Moreno, J. I., & Vicente-Serrano, S. M. (2012). Climate

896 change and its impact. In I. N. Vogiatzakis (Ed.), Mediterranean Mountain

897 Environments (pp. 185–201). Chichester, UK: Wiley-Blackwell.

898   Oksanen, J. (2015). Vegan: an introduction to ordination. URL http://cran.r-project.

899   org/web/packages/vegan/vignettes/introvegan. pdf, 8, 19.

900   Oliva, M., Gómez-Ortiz, A., Salvador-Franch, F., Salvà-Catarineu, M., Palacios, D.,

901   Tanarro, L., ... & Ruiz-Fernández, J. (2016). Inexistence of permafrost at the top

902   of the Veleta peak (Sierra Nevada, Spain). Science of the Total Environment, 550,

903   484-494.

904   Palomo, I., Martín-López, B., Potschin, M., Haines-Young, R., & Montes, C. (2013).

905   National Parks, buffer zones and surrounding lands: mapping ecosystem service

906   flows. Ecosystem Services, 4, 104-116.

907   Paull, T. M., Finkelstein, S. A., & Gajewski, K. (2017). Interactions between climate

908   and landscape drive Holocene ecological change in a High Arctic lake on

909   Somerset Island, Nunavut, Canada. Arctic Science, 3, 17-38.

910   Pérez-Luque, A. J., Pérez-Pérez, R., & Bonet, F. J. (2016). Climate change over the last

911   50 years in Sierra Nevada, in: Global Change Impacts in Sierra Nevada:

912   Challenges for conservation, Zamora, R., Pérez-Luque, A. J., Bonet, F. J., Barea-

913   Azcón, J. M., Aspizúa R. (Coords), pp. 24-26, Consejería de Medio Ambiente y

914   Ordenación del Territorio, Junta de Andalucía.

915   Pérez-Martínez, C., Barea-Arco, J., Conde-Porcuna, J. M., & Morales-Baquero, R.

916   (2007). Reproduction strategies of *Daphnia pulicaria* population in a high

917   mountain lake of Southern Spain. Hydrobiologia, 594, 75-82.

918   Pérez-Martínez, C., Conde-Porcuna, J. M., Moreno, E., Ramos-Rodríguez & Jiménez,

919   L. (2020) Cladoceran assemblage distribution in shallow alpine lakes of Sierra

920   Nevada (Spain) and its relationship with environmental variables. Aquatic

921   Sciences, 82, 4. doi: 10.1007/s00027-019-0677-5.

922 Pérez-Martínez, C., Jiménez, L., Moreno, E., & Conde-Porcuna, J. M. (2013).

923 Emergence pattern and hatching cues of *Daphnia pulicaria* (Crustacea,

924 Cladocera) in an alpine lake. Hydrobiologia, 707, 47-57.

925 Pérez-Palazón, M. J., Pimentel, R., Herrero, J., Aguilar, C., Perales, J. M., & Polo, M. J.

926 (2015). Extreme values of snow-related variables in Mediterranean regions: trends

927 and long-term forecasting in Sierra Nevada (Spain). Proceedings of the

928 International Association of Hydrological Sciences, 369, 157-162.

929 Pey, J., Querol, X., Alastuey, A., Forastiere, F., & Stafoggia, M. (2013). African dust

930 outbreaks over the Mediterranean Basin during 2001–2011: PM10 concentrations,

931 phenomenology and trends, and its relationwith synoptic and mesoscale

932 meteorology. Atmospheric Chemistry and Physics, 13, 1395–1410.

933 Preston, D. L., Caine, N., McKnight, D. M., Williams, M. W., Hell, K., Miller, M. P., ...

934 & Johnson, P. T. (2016). Climate regulates alpine lake ice cover phenology and

935 aquatic ecosystem structure. Geophysical Research Letters, 43(10), 5353-5360.

936 Prospero, J. M., & Lamb, P. J. (2003). African droughts and dust transport to the

937 Caribbean: Climate change implications. Science, 302 (5647), 1024-1027.

938 Puga, E., Díaz de Federico, A., Nieto, J. M., & Díaz Puga, M. A. (2007). Petrología,

939 evolución geodinámica y georrecursos del Espacio Natural de Sierra Nevada.

940 Estudios Geológicos, 63, 19–40.

941 Pulido-Villena, E., Reche, I., & Morales-Baquero, R. (2006). Significance of

942 atmospheric inputs of calcium over the southwestern Mediterranean region: High

943 mountain lakes as tools for detection. Global Biogeochemical Cycles, . 20,

944 GB2012,doi:10.1029/2005GB002662.

945   R Development Core Team (2015). R: A Language and Environment for Statistical

946   Computing http://www. R-project. org.

947   Rivera-Rondón, C. A., & Catalan, J. (2019). Diatoms as indicators of the multivariate

948   environment of mountain lakes. Science of The Total Environment, 703, 135517.

949   https://doi.org/10.1016/j.scitotenv.2019.13551

950   Reche, I., Ortega-Retuerta, E., Romera, O., Villena, E. P., Baquero, R. M., &

951   Casamayor, E. O. (2009). Effect of Saharan dust inputs on bacterial activity and

952   community composition in Mediterranean lakes and reservoirs. Limnology and

953   Oceanography, 54, 869-879.

954   Reche, I., Pulido-Villena, E., Conde-Porcuna, J. M., & Carrillo, P. (2001).

955   Photoreactivity of dissolved organic matter from high-mountain lakes of Sierra

956   Nevada, Spain. Arctic, Antarctic, and Alpine Research, 33, 426-434.

957   Reche, I., Pulido-Villena, E., Morales-Baquero, R., & Casamayor, E.O. (2005). Does

958   ecosystem size determine aquatic bacterial richness? Ecology, 86, 1715-1722.

959   Ridame, C., & Guieu, C. (2002). Saharan input of phosphate to the oligotrophic water

960   of the open western Mediterranean Sea. Limnology and Oceanography, 47(3),

961   856-869.

962   Rodá, F., Bellot, J., Ávila, A., Escarré, A., Piñol, J., & Terradas, J. (1993). Saharan dust

963   and the atmospheric inputs of elements and alkalinity to Mediterranean

964   ecosystems. Water, Air, and Soil Pollution, 66(3-4), 277-288.

965   Rogora, M., Frate, L., Carranza, M. L., Freppaz, M., Stanisci, A., Bertani, I., ... &

966   Cerrato, C. (2018). Assessment of climate change effects on mountain ecosystems

967   through a cross-site analysis in the Alps and Apennines. Science of the Total

968   Environment, 624, 1429-1442. https://doi.org/10.1016/j.scitotenv.2017.12.155

969   Round F. E., Crawford E. M., & Mann, D.G. (1990). The Diatoms. Cambridge
970   University Press, Cambridge, 747 pp.

971   Rühland, K. M., & Smol, J. P. (2002). Freshwater diatoms from the Canadian arctic
972   treeline and development of paleolimnological inference models. Journal of
973   Phycology, 38(2), 249-264.

974   Rühland, K.M., Paterson, A.M., & Smol, J.P. (2015) Diatom assemblage responses to
975   warming: reviewing the evidence. Journal of Paleolimnology 54: 1-35.

976   Ruiz-Sinoga, J. D., Garcia-Marin, R., Martinez-Murillo, J. F., & Gabarron-Galeote, M.
977   A. (2011). Precipitation dynamics in southern Spain: trends and cycles.
978   International Journal of Climatology, 31, 2281-2289.

979   Sánchez-Castillo, P., Linares-Cuesta, E., & Fernández Moreno, D. (2008). Changes in
980   epilithic diatom assemblages in a Mediterranean high mountain lake (Laguna de
981   La Caldera, Sierra Nevada, Spain) after a period of drought. Journal of
982   Limnology, 67, 49-55. 10.4081/jlimnol.2008.49.

983   Sánchez-López , G., Hernández, A., Pla-Rabes, S., Toro, M., Granados, I., Sigrò, J.,
984   Trigo, R. M., Rubio-Inglés, M. J., Camarero, L., Valero-Garcé,s B. & Giralt, S.
985   (2015). The effects of the NAO on the ice phenology of Spanish alpine lakes.
986   Climatic Change, 130, 101-113.

987   Schelske, C. L., Peplow, A., Brenner, M., & Spencer, C. N. (1994). Low-background
988   gamma counting: applications for 210 Pb dating of sediments. Journal of
989   Paleolimnology, 10, 115-128.

990   Siver, P. A., & Baskette, G. (2004). A morphological examination of Frustulia
991   (Bacillariophyceae) from the Ocala National Forest, Florida, USA. Canadian
992   Journal of Botany, 82, 629-644.

993   Smol, J. P. (2008). Pollution of lakes and rivers: a paleoenvironmental perspective. John

994   Wiley & Sons.

995   Sochuliaková, L., Sienkiewicz, E., Hamerlík, L., Svitok, M., Fidlerová, D., & Bitušík,

996   P. (2018). Reconstructing the trophic history of an alpine lake (High Tatra Mts.)

997   using subfossil diatoms: disentangling the effects of climate and human influence.

998   Water, Air, & Soil Pollution, 229(9), 289.

999   Sorvari, S, Korhola, A., & Thompson, r. (2002). Lake Diatom Response to Recent

1000   Arctic Warming in Finnish Lapland. Global Change Biology, 8, 171–181.

1001   Steinbauer, M. J., Grytnes, J. A., Jurasinski, G., Kulonen, A., Lenoir, J., Pauli, H., ... &

1002   Bjorkman, A. D. (2018). Accelerated increase in plant species richness on

1003   mountain summits is linked to warming. Nature, 556 (7700), 231.

1004   Summers, J. C., Kurek, J., Rühland, K. M., Neville, E. E., & Smol, J. P. (2017).

1005   Assessment of multi-trophic changes in a shallow boreal lake simultaneously

1006   exposed to climate change and aerial deposition of contaminants from the

1007   Athabasca Oil Sands Region, Canada. Science of the Total Environment, 592,

1008   573-583.

1009   Toms, J. D., & Lesperance, M. L. (2003). Piecewise regression: a tool for identifying

1010   ecological thresholds. Ecology, 84(8), 2034-2041.

1011   Udelhoven, T., Stellmes, M., del Barrio, G., & Hill, J. (2009). Assessment of rainfall

1012   and NDVI anomalies in Spain (1989–1999) using distributed lag models.

1013   International Journal of Remote Sensing, 30, 1961–1976.

1014   Vadeboncoeur, Y., Jeppesen, E., Zanden, M. J. V., Schierup, H. H., Christoffersen, K.,

1015   & Lodge, D. M. (2003). From Greenland to green lakes: cultural eutrophication

and the loss of benthic pathways in lakes. Limnology and oceanography, 48, 1408-1418.

Vadeboncoeur, Y., Devlin, S. P., McIntyre P.B., & Van der Zanden, M.J. (2014). Is there light after depth? Distributionof periphyton chlorophyll and productivity in lake littoral zones. Freshwater Science, 33, 524–36

Van De Vijver, B., Frenot, Y., & Beyens, L. (2002). Freshwater diatoms from Ile de la Possession (Crozet Archipelago, Subantarctica).Bibliotheca Diatomologica, 46, 1-412. J. Cramer, Berlin Stuttgart.

Villar-Argaiz, M., Medina-Sánchez, J. M., Cruz-Pizarro, L., & Carrillo, P. (2001). Inter-and intra-annual variability in the phytoplankton community of a high mountain lake: the influence of external (atmospheric) and internal (recycled) sources of phosphorus. Freshwater Biology, 46, 1017-1034.

Vinocur, A., & Maidana, N. I. (2010). Spatial and temporal variations in moss-inhabiting summer diatom communities from Potter Peninsula (King George Island, Antarctica). Polar Biology, 33, 443-455.

Weckström, J., Korhola, A., & Blom, T. (1997). Diatoms as quantitative indicators of pH and water temperature in subarctic Fennoscandian lakes. Hydrobiologia, 347, 171-184.

Wilson, S.E., Cumming, B.F., & Smol, J.P. (1996). Assessing the reliability of salinity inference models from diatom assemblages: an examination of a 219-lake data set from western North America. Canadian Journal of Fisheries and Aquatic Sciences, 53, 1580-1594.

1040 **Table 1**. Summary of results from the model selection analyses predicting the DCA axis

1041 1 and axis 2 scores of the diatom assemblages for each of the study lakes. The

1042 explanatory variables were z-score transformed to standardize to mean variance.

1043

Lake	Response variable		Regression Model	Adj R^2	F	AICc
RS	DCA axis 1	1	-0.0013 + 0. 412***Temp - 0.154**SPI - 0.078§wNAO	0.905	58.12	-6.9
		2	-0.0013 + 0.40***Temp - 0.13*SPI	0.888	72.45	-6.3
RSS	DCA axis 1		Null model			
AV	DCA axis 1	1	-0.0269 - 0.1875***Temp	0.674	54.75	-21.6
		2	0.02629 - 0.18607***Temp + 0.1511^{ns}Precip	0.665	26.83	-20.3
BG	DCA axis 1	1	-0.02171 - 0.1504***Temp + 0.1019***SPI	0.817	50.19	14.9
MC	DCA axis 1	1	-0.0098 - 0.2018***Temp	0.886	136.1	-19.1
		2	0.0022 - 0.2161***Temp - 0.043*wNAO	0.846	55.86	-17.5
CD	DCA axis 1	1	-0.04832 + 0.16522***Temp	0.614	45.58	-14.0

1044
1045
1046 Lake name abbreviations: Río Seco (RS), Río Seco Superior (RSS), Aguas Verdes (AV), Borreguil (BG), Mosca (MC), and Cuadrada (CD).
1047 The best models according to the Akaike's information criterion (AICc) values for the DCA are shown. One to three outliers were removed
1048 in analyses of DCA 1 in MC and CD and DCA 2 in MC, but similar results were obtained when they were included. Predictor variables for
1049 both analyses include: Temp, Madrid air temperature; Precip, San Fernando precipitation; SPI, Sahel precipitation index; wNAO, winter
1050 NAO index.
1051 Adj R_2, adjusted R_2.
1052 Significance levels: ***$p < .001$; **$.001 < p < .01$; *$.01 < p < .05$; $_\S.05 < p < .1$; $_{ns} p > .1$.
1053

Table 2. Summary of results from the model selection analyses predicting the relative abundance of *S. pinnata* for five of the study lakes and of *A. alpigena* for RS Lake. The explanatory variables were z-score transformed to standardize to mean variance.

Lake	Response variable		Regression Model	Adj R^2	F	AICc
RS	*S. pinnata*	1	3.3753 + 2.6467***Temp - 1.5159*SPI	0.742	25.47	84.9
	A. alpigena	1	14.483 -6.817*Temp + 8.738**Precip + 3.305[ns]wNAO	0.437	6.95	193.3
		2	14.331 - 6.187*Temp + 7.073*Precip	0.413	9.09	194.3
RSS	*S. pinnata*	1	92.2977 -1.1667**Precip -0.7939[§]wNAO	0.124	2.90	142.4
AV	*S. pinnata*	1	61.445 + 9.960***Temp - 2.473[§]Precip	0.637	25.59	207.7
		2	61.610 + 10.367***Temp	0.613	45.36	207.9
BG	*S. pinnata*	1	2.4979 + 0.8259**Temp -0.7707**SPI	0.562	17.05	88.3
MC	*S. pinnata*	1	4.0635 + 2.7397***Temp + 1.0133**wNAO	0.721	28.09	89.7

Lake name abbreviations: Río Seco (RS), Río Seco Superior (RSS), Aguas Verdes (AV), Borreguil (BG), Mosca (MC), and Cuadrada (CD).
The best models according to the Akaike's information criterion (AICc) values for the DCA are shown. One to two outliers were removed in analyses of *S. pinnata* in RS, AV, and MC, but similar result were obtained when they were included. Predictor variables for both analyses include: Temp, Madrid air temperature; Precip, San Fernando precipitation; SPI, Sahel precipitation index; wNAO, winter NAO index.
Adj R$_2$, adjusted R$_2$.
Significance levels: ***p < .001; **.001 < p < .01; *.01 < p < .05; $_§$.05 < p < .1; $_{ns}$ p > .1.

Figure 1. a) Map of Europe and map of the Iberian Peninsula showing the location of the study area. b) Map of the Sierra Nevada mountain range. c) Geographic locations of the six study lakes (circles), from left to right: Cuadrada (CD), Aguas Verdes (AV), Río Seco Superior (RSS), Río Seco (RS), Mosca (MC), Borreguil (BG).
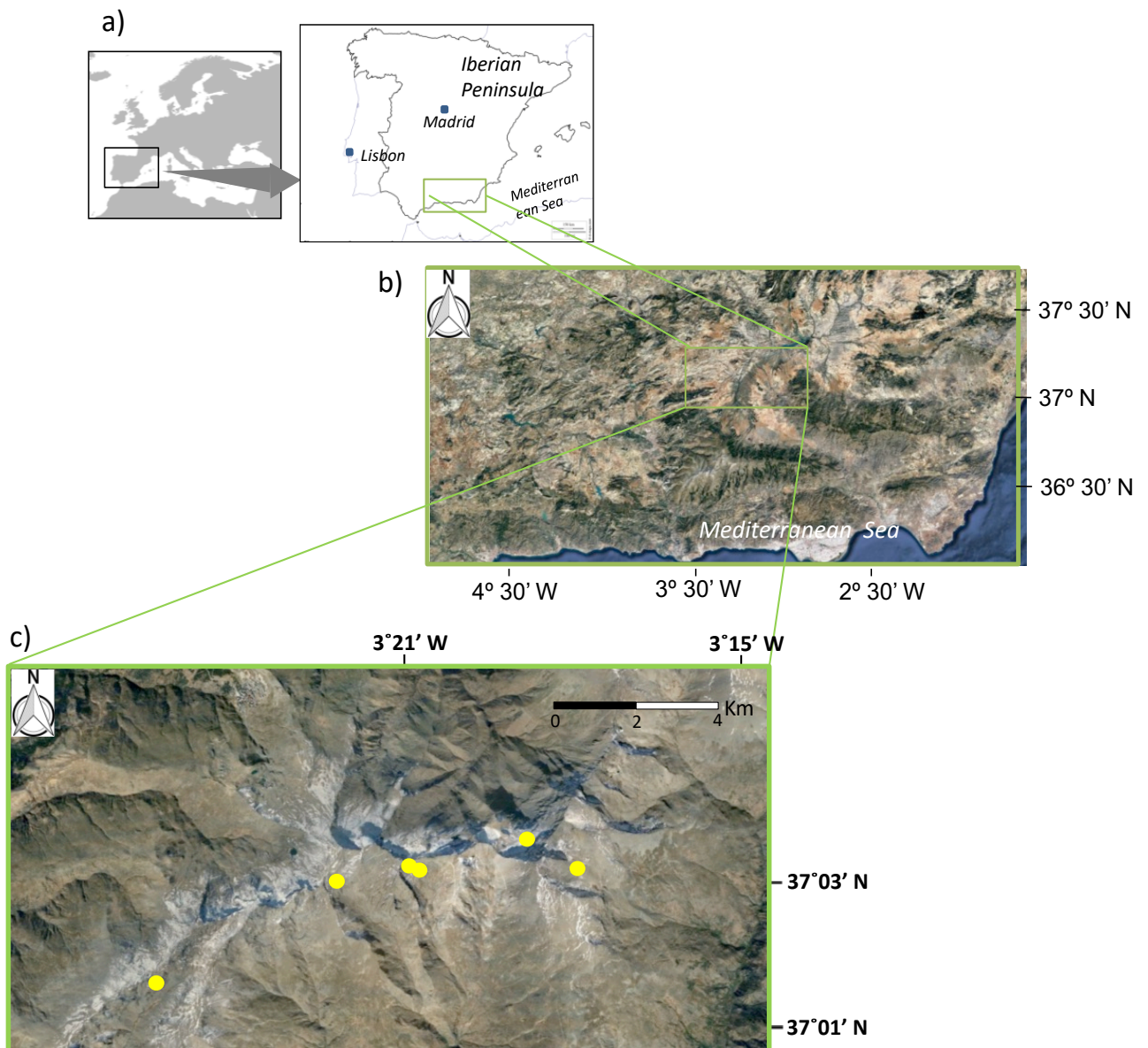
1079 **Figure 2.** Historical trends of the mean annual air temperature anomaly from the

1080 Madrid climate station (MAAT Madrid), the annual precipitation anomaly from the San

1081 Fernando climate station (AP San Fernando), the Sahel precipitation index (SPI) and the

1082 wNAO index. Temperature anomalies are calculated from the period 1961 to 1990 and

1083 precipitation anomalies are calculated over the entire period. The anomalies of the SPI

1084 are calculated with respect to 1900 and 2013, and based on June through October

1085 averages for each year. A LOESS smoother (span = 0.2) was applied to all the variables

1086 to improve the clarity of the figure and highlight trends. The temperature series

1087 breakpoint is shown.
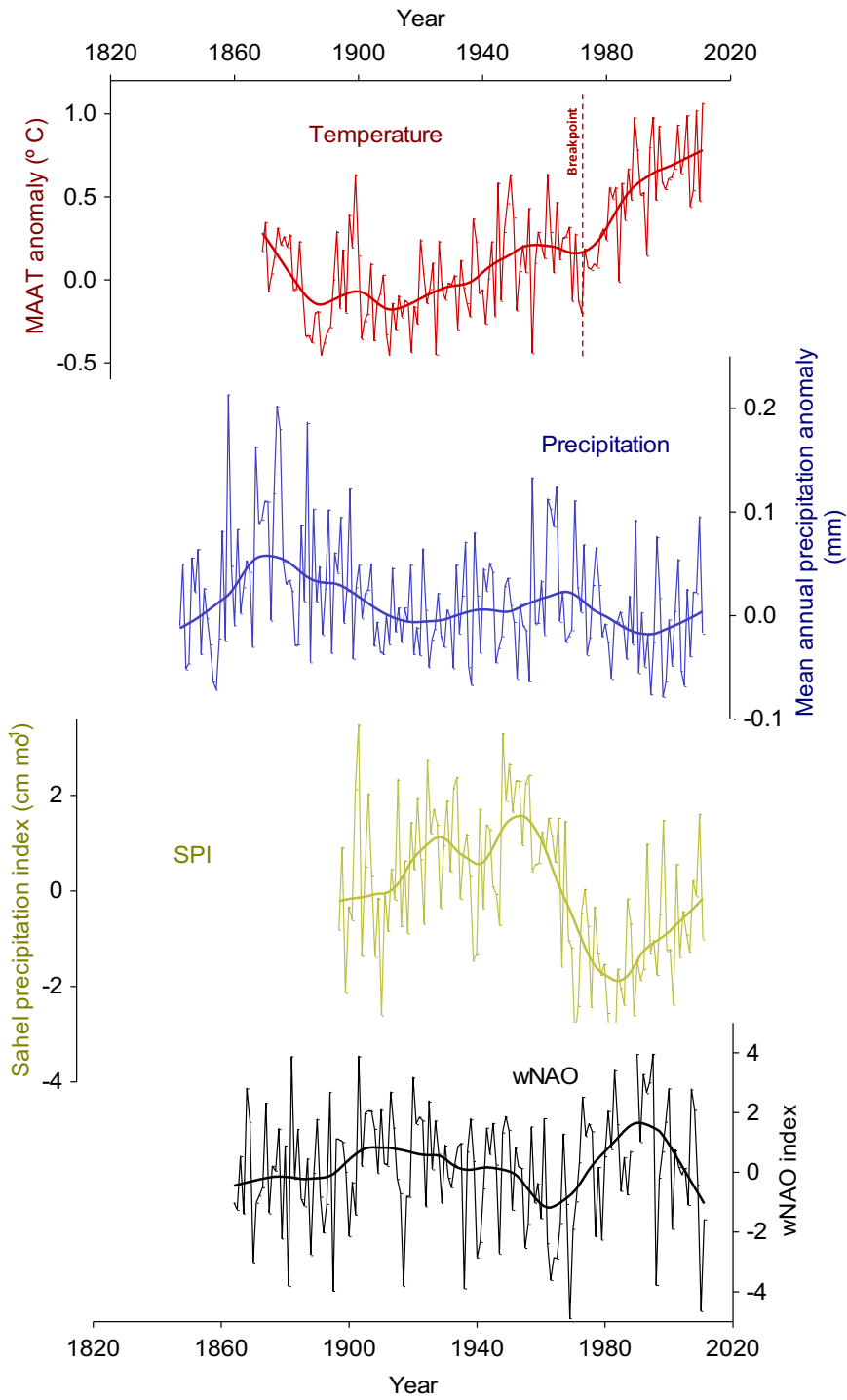
1088

1089

1090

1091

1092

1093

51

1094   **Figure 3.** Relative frequency diagrams of the most common diatom taxa (taxa with

1095   relative abundance >1% in at least one sediment sample interval) recorded in the

1096   sediment cores from the six study lakes. The broken line represents the main zonation

1097   identified by the broken stick model. Groupings include the *Encyonema* complex (*E.*

1098   *minutum, E. perpusillum, E. silesiacum*), the *Eunotia* complex (*E. bilunaris, E. diodon,*

1099   *E. glacialis, E. incisa, E. minor, E. silesiacum, E. tenella*), the *Gomphonema* complex

1100   (*G. clavatum, G. exilissimum, G. gracile, G. parvulum*), and the *Pinnularia* complex (*P.*

1101   *borealis, P. julma, P. maior, P. microstauron, P. perirrorata, P. pseudacuminata, P.*

1102   *sinistra, P. viridis*).

1103

1104

1105

1106
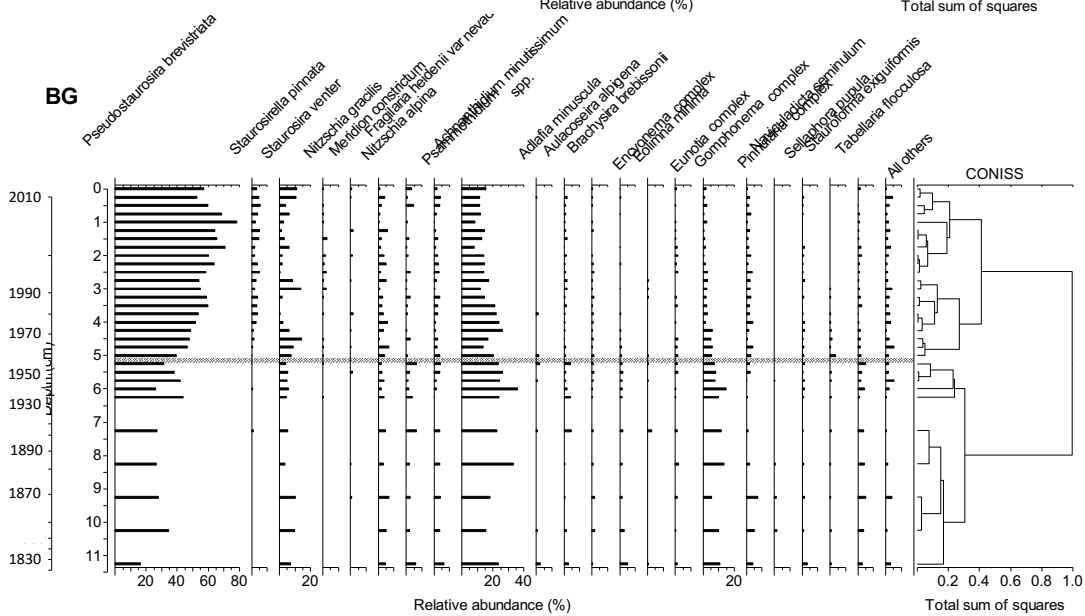
1107

1108

1109

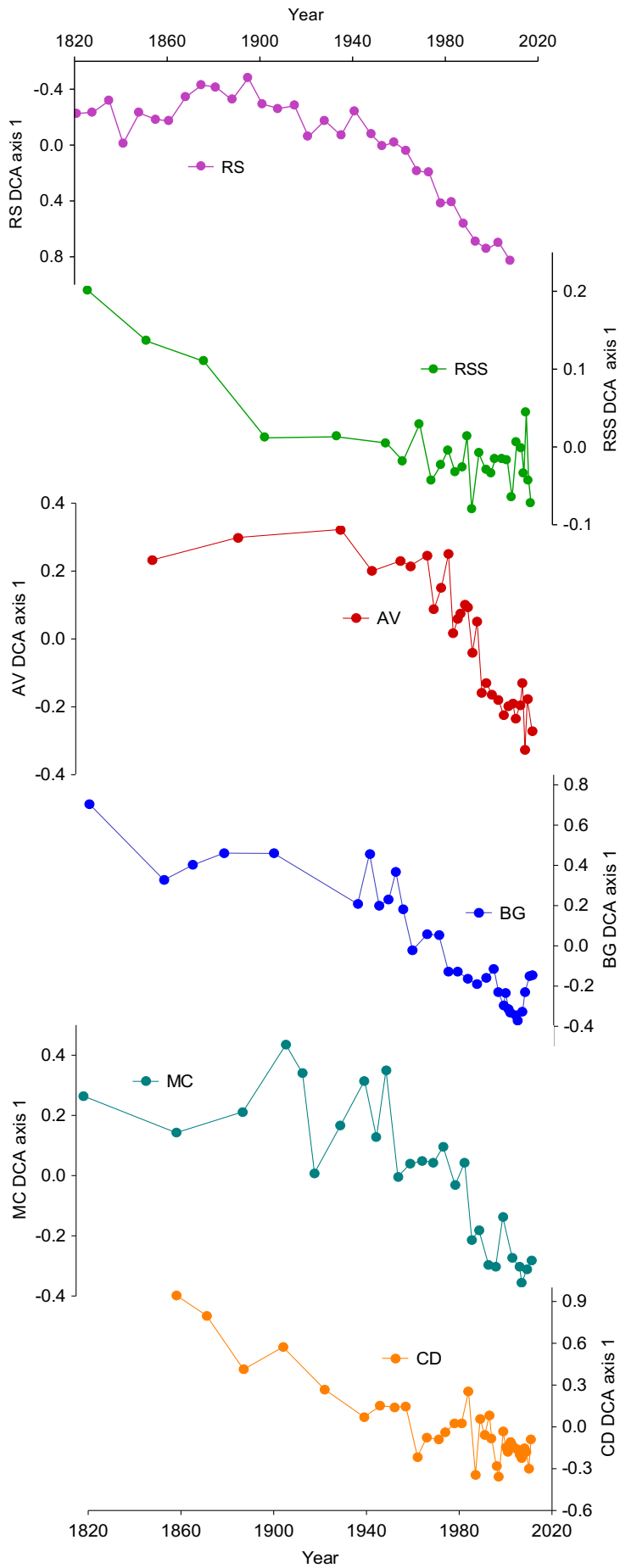1110

1111
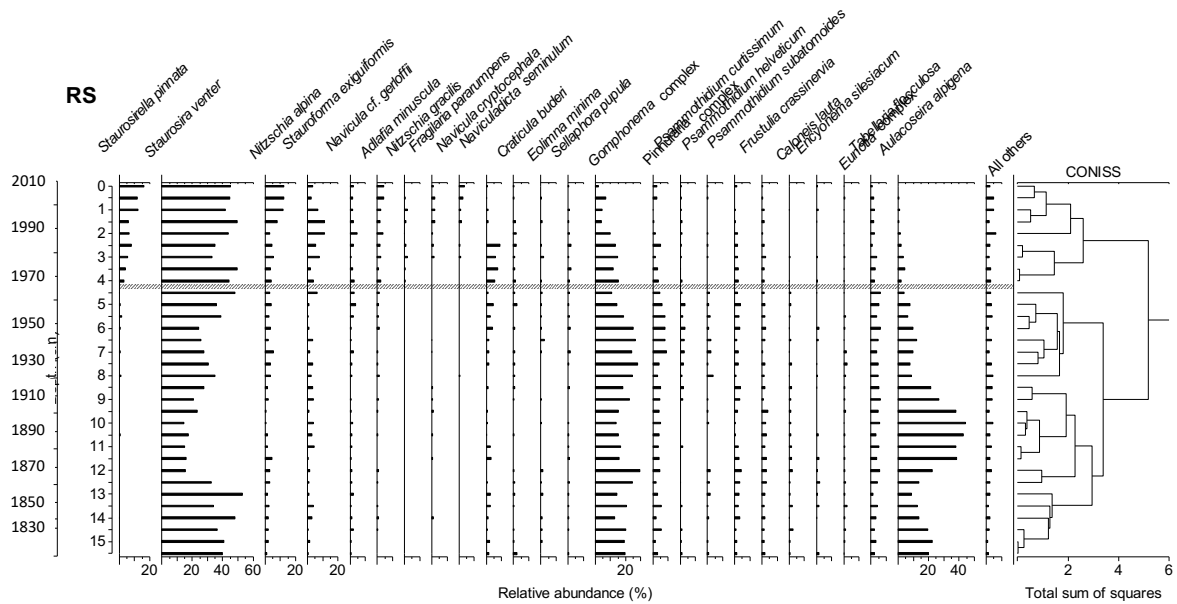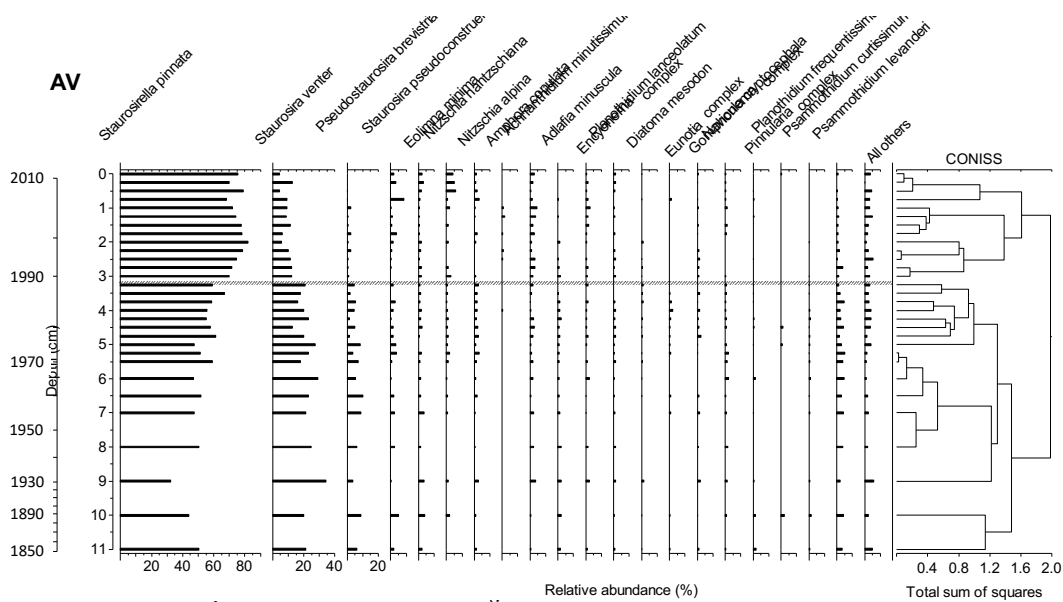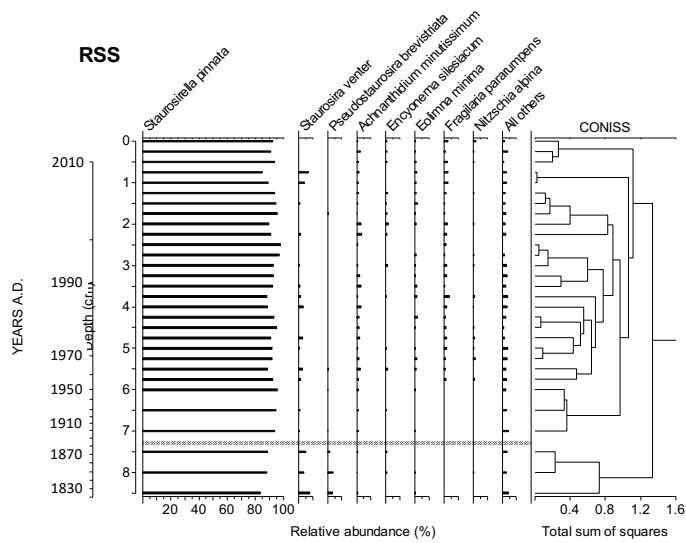
1112 **Figure 4.** Detrended correspondence analysis (DCA) axis 1 sample scores for diatom

1113 assemblages plotted against estimated ^{210}Pb dates for the six study lakes. Lake name

1114 abbreviations: Río Seco (RS), Río Seco Superior (RSS), Aguas Verdes (AV), Borreguil

1115 (BG), Mosca (MC) and Cuadrada (CD).

1116

Supplementary material for

Long-term ecological changes in Mediterranean mountain lakes linked to recent climate change and Saharan dust deposition revealed by diatom analyses

Carmen Pérez-Martínez[1,2], Kathleen M. Rühland[3], John P. Smol[3], Vivienne J. Jones[4] and José M. Conde-Porcuna[1,2]

[1]Institute of Water Research, University of Granada, 18071-Granada, Spain

[2]Department of Ecology, Faculty of Science, University of Granada, 18071-Granada, Spain

[3]Paleoecological Environmental Assessment and Research Lab (PEARL), Department of Biology, Queen's University, Kingston, ON K7L 3N6, Canada

[4]Environmental Change Research Centre, Department of Geography, University College London, Pearson Building, Gower Street, London, WC1E 6BT, U.K.

Corresponding author: Carmen Pérez-Martínez, cperezm@ugr.es

1140

1141

1142

1143 **Supplementary Table S1**. Location and environmental characteristics of the six study

1144 lakes in Sierra Nevada Mountains. Range and mean values or single values of the

1145 chemical and biological parameters from water column measurements are shown.

1146

LAKES	Río Seco (RS)	Río S. Superior (RSS)	Aguas Verdes (AV)	Borreguil (BG)	Mosca (MC)	Cuadrada (CD)
Latitude	37º03'07.63''N	37º03'06.69''N	37º02'54.79''N	37º03'09.53''N	37º03'35.03''N	37º01'37.18''N
Longitude	3º20'43.92''W	3º20'53.04''W	3º22'06.16''W	3º17'59.03''W	3º18'53.03''W	3º25'06.64''W
Altitude (m asl)	3020	3040	3050	2980	2920	2840
Lake Area (ha)[a]	0.42	0.07	0.19	0.18	0.44	0.24
Catchment area (ha)[a]	9.9	4.7	12.8	50.9	39.7	4.0
Maximum depth (m)	2.9	2.6	2.8	2.0	2.8	4.8
Maximum volume (m^3)[b]	4772	447	1262	2070	7044	-
Catchment area/surface area[a]	21.5	78.3	67.4	282.8	82.7	16.7
Meadowarea (ha)	0.91	0.02	0.31	0.55	0.25	0.05
Meadowarea/Lake area	2.17	0.29	1.63	3.06	0.57	0.11
pH	6.0-7.6 (6.9)	6.4-7.8 (7.2)	6-7.2 (6.7)	6.3	7.5-7.8 (7.7)	7.7
Conductivity (µS cm^{-1})	10-77 (24)	14-17 (15)	25-30 (27)	13-15 (14)	27-37 (32)	6-9 (7)
Alkalinity (meq L^{-1})	0.55-0.16 (0.11)	0.14-0.17 (0.16)	0.07-0.23 (0.16)	0.07-0.1 (0.09)	1.57	009-0.20 (0.14)
TP (µg L^{-1})	7-27 (16)	13-17 (15)	12-28 (20)	13-27 (18)	11-28 (17)	8-11 (9)
TN (µg L^{-1})	99-732 (403)	133-435 (284)	216-251 (236)	180-380 (280)	268-308 (288)	41-126 (83)
DSi (mg L^{-1})	0.66-0.12 (0.32)	0.33-0.54 (0.42)	0.53-0.69 (0.60)	0.57-0.38 (0.48)	0.88-0.91 (0.90)	0.25-0.26 (0.26)
Chl*a* (µg L^{-1})	0.3-1.1 (0.6)	0.6-2.1 (1.2)	0.6-1.1 (0.8)	1.4-1.7 (1.5)	0.04-2.1 (1.1)	0.5-1.8 (1.1)
DOC (mg L^{-1})	0.7-2.7 (1.8)	0.9-1.3 (1.1)	0.7-1.2 (1.0)	0.6-1.1 (0.9)	1.1-1.4 (1.2)	0.5-1.3 (0.7)
Calcium (mg L^{-1})	0.5-2.1 (1.2)	0.5-2.8 (1.9)	1.9-2.1 (2.0)	0.8-1.1 (1.0)	3.0-6.6 (5.0)	0.3-1.1 (0.6)

1147
1148 TP, Total phosphorus; TN, Total nitrogen; DSi, Dissolved silica;Chl*a*, Chlorophyll-*a;* DOC, Dissolved Organic Carbon.
1149 Chemical and biological characteristics are from Sánchez-Castillo *et al*. (1989), Morales-Baquero *et al*. (1999), Reche*et al*. (2005) as well as from
1150 water column samples taken during each core sampling day and for punctual subsequent samples. Data are derived from a monitoring study over the
1151 past 10 years in RS Lake and for punctual samplings in RSS, AV, BG, MC and CD Lakes. Range and mean values are from a minimum of four
1152 samples for RSS and AV, three for BG, two for MC and six for CD Lake.
1153 [a] Data from Morales-Baquero *et al*. (1999).
1154 [b] Data from Egmasa S.A.

1155

1156

1157

1158

1159

1160 **Supplementary Table S2**. Relative abundances of diatom genera showing more than

1161 5% of relative abundance in samples of epiphyton in Río Seco (RS) and Mosca (MC)

1162 lake meadows. *Achnanthidium* is mainly composed of *A. minutissimum, Encyonema* by

1163 *E. minutum*, *Eunotia* by *E. tenella*, *Gomphonema* by *G. exilissimum* (in RS), *Nitzschia*

1164 by *N. alpina* and *Pinnularia* by *P. sinistra* and *P. microstauron.*

1165
1166

|	*Achnanthidium*	*Encyonema*	*Eunotia*	*Gomphonema*	*Nitzschia*	*Pinnularia*
Río Seco (RS)	0	0	65.0	7.2	6.1	11.7
Mosca (MC)	70.3	9.0	0	6.0	5.1	0

1167

1168

1169

1170 **Supplementary Figure S1**. Pictures of the selected six study lakes (the date each

1171 picture was taken is specified). Source: https://lagunasdesierranevada.es/. Picture´s

1172 authors: RS, AV and RSS: Eulogio Corral Arredondo, BG: Jesús Fernández Cuerpo,

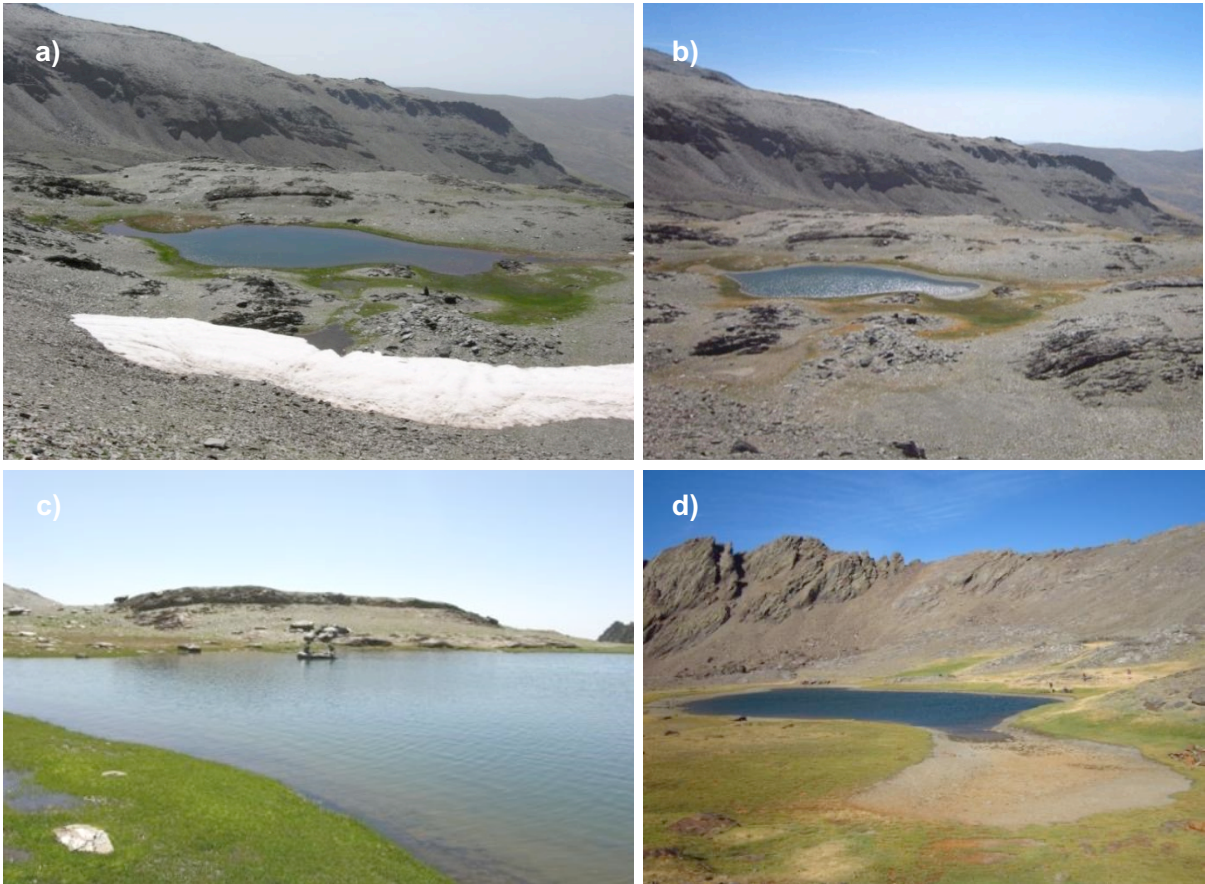1173 MC: José Ignacio Cuenca and CD: Víctor Cassini.

1174

1175
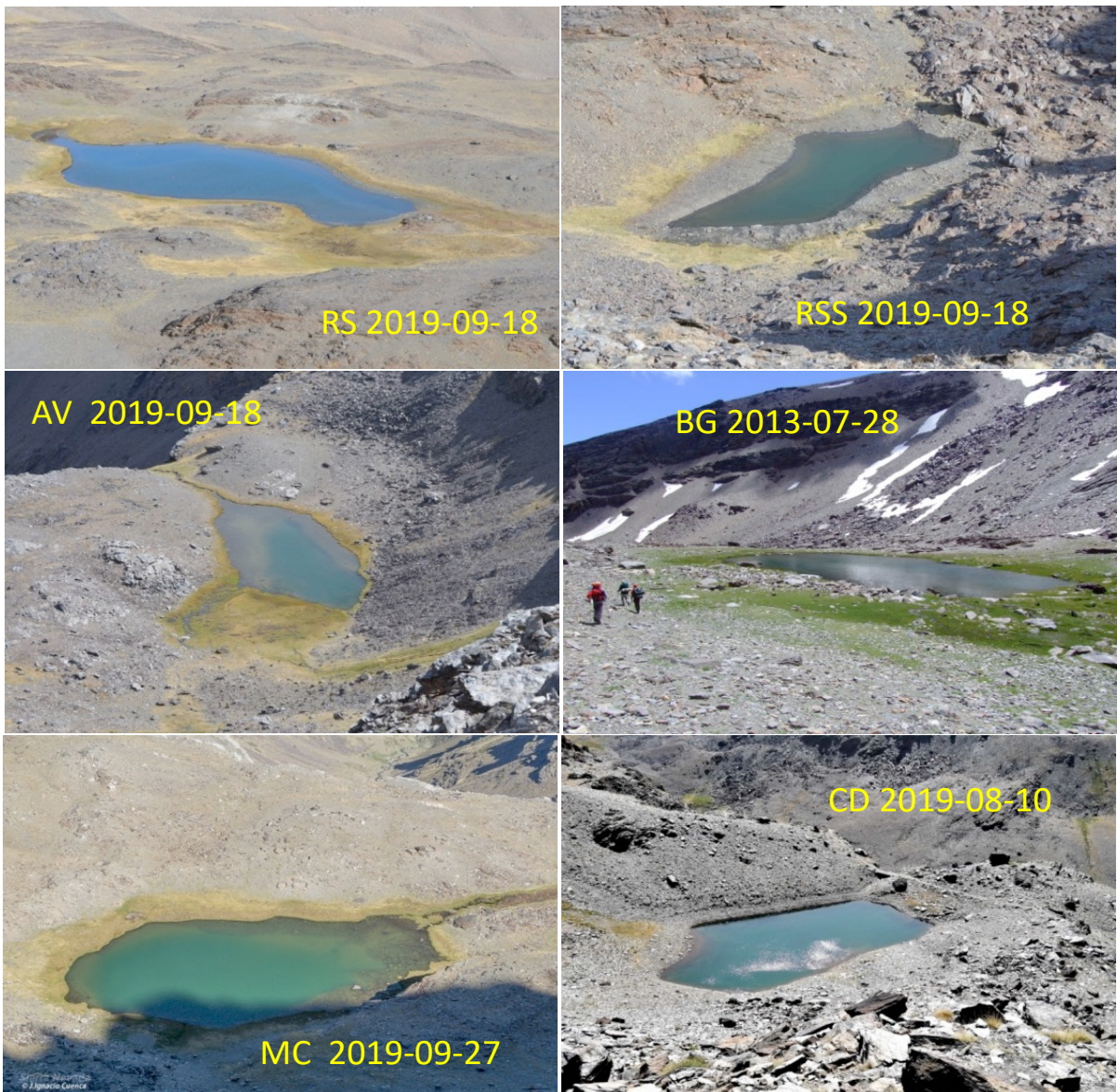
1176

1177

1178   **Supplementary Figure S2.** a-d) Images of RS Lake in a wet and cold year (2010) and

1179   during a drier and warmer year (2012); a) RS Lake on 26 August 2010, b) RS Lake on

1180   29 August 2012, c) Wet meadows in RS Lake on 26 August 2010, d) Dry meadows in

1181   RS Lake on 29 August 2012.

1182

1183

1184

1185

1186

1187 **Supplementary Figure S3.** Detrended correspondence analysis (DCA) axis 1 sample

1188 scores for diatom assemblages, principal component analysis (PCA) axis 1 scores for

1189 cladoceran assemblages and chlorophyll-*a* values plotted against estimated ^{210}Pb dates

1190 for the six study lakes. Z-scores of all the variables are shown. Lake name

1191 abbreviations: Río Seco (RS), Río Seco Superior (RSS), Aguas Verdes (AV), Borreguil

1192 (BG), Mosca (MC) and Cuadrada (CD).

1193